Reindeer in Space

Assessing the suitability of different satellite sensors to detect vegetation vulnerability to reindeer grazing patterns in East Iceland

Marteinn Möller

Faculty of Life and Environmental Sciences
University of Iceland
2021

Reindeer in Space

Assessing the suitability of different satellite sensors to detect vegetation vulnerability to reindeer grazing patterns in East Iceland

Marteinn Möller

10 ECTS thesis submitted in partial fulfilment of a *Baccalaureus Scientiarum* degree in Geography

Supervisor/s
Benjamin David Hennig
Noémie Boulanger-Lapointe

Faculty of Life and Environmental Sciences
School of Engineering and Natural Sciences
University of Iceland
Reykjavík, May 2021

Reindeer in Space
Assessing the suitability of different satellite sensors to detect vegetation vulnerability to reindeer grazing patterns in East Iceland
10 ECTS thesis submitted in partial fulfilment of a *Baccalaureus Scientiarum* degree in Geography

Faculty of Life and Environmental Sciences
School of Engineering and Natural Sciences
University of Iceland
Askja, Sturlugata 7
101, Reykjavik
Iceland

Telephone: 525 4000

Bibliographic information:
Marteinn Möller, 2021, Reindeer in space: Assessing different satellite's capability to detect reindeer grazing patterns in East Iceland, BS thesis, Faculty of Life and Environmental Sciences, University of Iceland, pp. 44.

Printing: Háskólaprent
Reykjavik, Iceland, May 2021

Abstract

The impact of sheep on soil erosion in Iceland is widely acknowledged as a central element of the process, while wildlife grazing pressure has been left largely unexplored. Novel metabolic biomass data of reindeer (*Rangifer tarandus*) in Iceland, including their modelled spatial distribution, can be used as a predictor of reindeer presence and related to their grazing pressure. In this study, I used the NDVI extracted from four different publicly available satellite products as a predictor of forage availability and compared it to the reindeer's biomass data to determine whether particular areas were more vulnerable than others to reindeer overgrazing. To do so, I calculated a grazing vulnerability index and used it to create four maps of a sample area in Úthérað (East Iceland), highlighting areas at risk of overgrazing. The satellites have different sensors, and the results differed due to the varying spatial– and temporal resolution component of each sensor. The sensors with high spatial resolution were capable of measuring details that were not detectable on the other sensors, but they also had a low temporal resolution making them susceptible to cloud–cover. The sensors with high temporal resolution had a low spatial resolution making them less compatible for detailed observations. However, their high temporal resolution combined with multi–day composite products made the NDVI product more reliable. The data was also smaller in size, causing them to be less computational resource intensive. The high temporal resolution data were thus, determined more suitable for large scale vulnerability measures.

Útdráttur

Jarðvegseyðing af völdum ofbeitar á Íslandi hefur hlotið þónokkra athygli vísindamanna. Áhrif sauðfjárbeitar á ferlið er viðurkennd sem ein af megin orsökum jarðvegseyðingar á meðan hlutur villtra dýra er lítt þekkt stærð. Ný gögn sem sýna lífmassa–efnaskipti hreindýra á Íslandi og líkja eftir dreifingu þeirra má nýta sem fyrirboða á viðveru þeirra á ákveðnu svæði. Gögnin innihalda staðsetningu í formi rasta og líkja eftir beitarálagi hreindýra. Gróðurstuðull var notaður sem fyrirboði á framboði fóðurs sem borið var saman við lífmassa gögn hreindýra og með því ákvarðað hvar hætta á ofbeit gat verið til staðar. Til þess voru gerð fjögur kort af úrtakssvæði í Úthéraði á Austurlandi sem sýna áhættusvæði fyrir ofbeit hreindýra. Kortin voru gerð úr ókeypis gögnum fjögurra mismunandi gervihnattamynda, aðgengilegum almenningi, með mismunandi nema. Gervihnettirnir leiddu af sér ólíkar niðurstöður vegna mismunandi upplausnar í nemunum það er rúm– og tímaupplausnar. Nemar með háa rúmupplausn sýndu smáatriði sem voru ómerkjanleg með lágri rúmupplausn en þeir höfðu lága tímaupplausn og voru því viðkvæmir fyrir skýjahulu. Nemar með háa tímaupplausn höfðu lága rúmupplausn og greindu því síður smáatriði en höfðu samsett gögn yfir tímabilið og voru því ónæmari fyrir skýjahulu. Þetta gerði þau áreiðanlegri og voru þau að auki minni að stærð og kröfðust þar af leiðandi minni reiknigetu. Há tímaupplausn var því ákvarðað sem ákjósanlegri eignileiki gagna fyrir víðtækar áhættu greiningar fyrir ofbeit.

Table of Contents

List of figures

List of Tables

Abbreviations

AVHRR	Advanced Very High Resolution Radiometer
BOA	Bottom Of Atmosphere
DPAS	Data Processing and Archive System
EOS	Earth Observing System
ESA	European Space Agency
ETM+	Enhanced Thematic Mapper Plus
fPAR	Fraction of Photosynthetically Active Radiation
GB	Gigabyte
GHZ	Gigahertz
GIS	Geographic Information System
HDF	Hierarchical Data Format
LAI	Leaf Area Index
LDCM	Landsat Data Continuity Mission
MODIS	Moderate Resolution Imaging Spectroradiometer
MSI	Multi−Spectral Instrument
NASA	National Aeronautics and Space Administration
NDVI	Normalised Difference Vegetation Index
NetCDF	Network Common Data Format
NIR	Near-Infrared Reflectance
NOAA	National Oceanic and Atmospheric Administration
OLCI	Ocean and Land Colour Instrument
OLI	Operational Land Imager
PDGS	Payload Data Ground Segment
RAM	Random–Access Memory
RED	Visible Red Light reflectance
SCP	Semi−Automatic Classification Plugin
SLSTR	The Sea and Land Surface Temperature Radiometer
SPOT	Satellite pour l'Observation de la Terre
SYN	Sentinel 3 Synergy
TIRS	Thermal Infrared Sensor
TM	Thematic Mapper
TOA	Top Of the Atmosphere
USGS	United States Geological Survey
VI	Vegetation Index

Acknowledgements

I would like to thank my supervisors Benjamin Hennig and Noémie Boulanger-Lapointe for their instructions and unbreakable patience. Their constructive critique was essential support for me through this process. I would also like to thank my friends and family for standing by me while I worked on the thesis, your tolerance does not come as a matter of course.

1 Introduction

Ecosystem responses to global environmental changes are a major focus of the scientific community (IPCC, 2014). The profound effect of human activity on ecosystems (e.g. via habitat degradation and biodiversity reduction) has increased the need to detect and predict future changes in ecosystems. In Iceland, poor land conditions and continued soil erosion are considered the most critical environmental problem today (Aradóttir & Arnalds, 2001; Arnalds, 2015; Arnalds et al., 2001). The highly erodible volcanic soils, harsh climatic conditions, and livestock grazing has led to severe soil erosion on about 40 % of the country's surface. Domestic sheep have been identified as the primary agent of land deterioration through intensive grazing, leading to biophysical changes in the vegetation cover.

The influence of wild herbivores, such as reindeer (*Rangifer tarandus*), is less studied in Iceland, likely due to their much lower numbers and limited range and remote habitats. Reindeer were introduced to Iceland by humans in 1787, with 35 domesticated reindeer brought from Norway. Their population has increased and dispersed around East Iceland and is still relatively low in number, about 6000 individuals. Today, they are only found in Eastern Iceland, where they migrate within a secluded area (Þórisson, 2018). Reindeer have no natural predators in Iceland to control their population. Therefore, good management is a prerequisite for them not to become invasive. Their grazing pressure on arctic biomes is not well documented, although Bernes et al. (2015) suggest a tendency for reindeer to overgraze low-productive sites.

Obtaining data for research focused on wild herbivores can be difficult due to their undomesticated nature and migratory behaviour. Field data is generally difficult to use for predicting regional or global changes because such data is traditionally collected at a small spatial and temporal scale (Newton et al., 2014; Pettorelli et al., 2005). To address this difficulty, remote sensing techniques are increasingly adopted by environmental scientists interested in predicting the effects of global warming, biodiversity reduction and habitat degradation.

Recent ecological studies using remote sensing techniques have highlighted the relevance of Vegetation Indices (VIs) to link vegetation and herbivore performance (Campeau et al., 2019; Newton et al., 2014; Pettorelli et al., 2005). Vegetation productivity and distribution are crucial to understanding herbivore distribution and dynamics. Empirical vegetation measurements on a grander scale − which are made possible by VIs − are vital to understanding trophic interactions (Beamish et al., 2020; Pettorelli et al., 2005). VIs enables ecologists to quantify how changes in vegetation, such as distribution and productivity, will affect upper trophic levels at different spatial scales. Therefore, VIs are helpful for monitoring ecosystem resilience by linking vegetation to animal performance.

This BS project is linked to ongoing research[1] at the University of Iceland and the Agricultural University of Iceland, which investigates the relationships between herbivore diversity and ecosystem functions, such as plant productivity, soil respiration and nutrient

[1] Herbivores in the tundra: linking diversity and function (Tundra Salad), Rannís project, 2021–2024

cycling, in the Icelandic highlands. The study compiles census and habitat preference data for the main herbivore species. In this project, I will contribute to this research by exploring tools that aid in evaluating the concentration of grazing and vegetation productivity.

1.1 Aims and objectives

There is a clear need to improve monitoring of the climate, vegetation and soil of the remote Icelandic highlands. This study compares imagery from two earth observation programs (Earth Observing System, or EOS, and Copernicus) and four satellite platforms (Sentinel 2 & 3, Landsat 8 and the Moderate Resolution Imaging Spectroradiometer, or MODIS) to evaluate the adequacy of using the normalised difference vegetation index (NDVI) as one of the commonly used VIs to detect reindeers' grazing stress on vegetation in east Iceland.

The aims of this study are:

(i) to assess the applicability of different satellite sensors to detect ecosystem vulnerability;

(ii) to present a method for assessing the impact of herbivores on vegetation by combining remote sensing techniques and species distribution data;

(iii) to establish procedures for a monitoring system to detect vulnerable areas to overgrazing;

(iv) to evaluate the utilisation of open data and open–source software for monitoring Iceland's ecosystems.

More specifically I will address the following objectives:

(a) to test the suitability of different satellite sensors for mapping the vegetation over the reindeer habitat;

(b) to discuss the compatibility of different satellite sensors to metabolic biomass data when investigating the risk of overgrazing;

(c) to discuss whether or when different satellite resolutions should take precedence for vegetation observations in Iceland specifically;

(d) to present an index that quantifies the vulnerability of habitats to impact from herbivores.

In this study, I will further advance our understanding of how the NDVI can be used to measure vegetation vulnerability in relation to reindeer grazing. Should there be areas at risk of overgrazing by reindeer, I highlight those areas by creating an index map to visualise them and relate them to their surroundings. Following this introduction, the theoretical framework behind similar studies will be covered in the literature review in Chapter 2. Chapter 3 will define and describe the material and methods used in the study. Results will be presented in Chapter 4 and discussed in Chapter 5 in the context of ongoing research and environmental management issues. My conclusions are presented in Chapter 6 where I offer recommendations for further research.

2 Literature review

Reindeer management in Iceland is closely linked to vegetation conditions due to the animals' impact on land degradation (Þórisson, 2018; Þórisson et al., 2021). The current population density benchmark is set at one animal per square kilometre of vegetated land in winter. Kristófersson et al. (2012) have proposed that fixed indicators of land condition should be established for monitoring temporal changes and conditions. Satellite images and remote sensing techniques have seen rapid advances in land degradation research (DeFries, 2013; Pettorelli et al., 2005). Specifically, the NDVI has proven to be a remarkably successful tool in scientific literature to understand changes in ecosystem conditions. Although several VIs have been developed, none have shown a significant advantage for phytomass estimations in tundra ecosystems in Iceland (Eckert & Engesser, 2013). Hence, due to its simplicity and accessibility, the NDVI was selected for this study. VIs and their previous uses will be described both functionally and their relationship with the reindeer population in the tundra ecosystem and the NDVI's performance and function with different satellite sensors.

2.1 Environmental and wildlife management in Iceland

In Iceland, formal wildlife management dates to 1849, with the first game legislation being introduced (Þórarinsson, 1950). In previous times the Grágás codex had some provision of animal numbers for the commons; however, not until 1940 were hunting regulations and monitoring efforts established for reindeer by the Ministry of Education and Culture. In 1990 wildlife management was transferred to the Ministry of Environment. Today the Environment Agency of Iceland (Umhverfisstofnun) operates under the Ministry of Environment which oversees the application of the Law on the Protection, Conservation and Hunting of Wild Birds and Mammals (Lög um vernd, friðun og veiðar á villtum fuglum og villtum spendýrum, 1994).

The current reindeer herd was introduced to Iceland in 1787 (Þórisson, 2018). Reindeer in Iceland have no natural predators and are not affected by exoparasitic insects like in other regions. Therefore, active management is necessary for the population not to become invasive. Current management is based on selective harvesting and regulated through the distribution of hunting quotas across nine hunting zones. Before introducing active management practices in the 20th century, food availability and weather were the main drivers of population dynamics. The population is currently increasing and milder climate conditions in East Iceland are believed to be driving those changes.

Overgrazing of the winter pastures in combination with harsh winters caused a drastic decline in population abundance in the late 19th century (Þórisson, 1983; Þórisson, 2018). Þórisson (2018) points out the necessity of evaluating the standing crop. He underlines that to estimate grazing pressure, the quantity and quality of plant species grazed and their standing crop in different habitats must be estimated, which is lacking for East Iceland. Following this recommendation, Kristófersson et al. (2012) made a new legislative proposal

to use fixed indicators for determining when the land conditions are deteriorating and setting management objectives for desirable vegetation condition. Currently, the set population density goal is one animal per kilometre squared of vegetated land in winter with six males per ten females (Þórisson, 2018).

2.2 Spaceborne remote sensing for environmental observations

Remote sensing techniques and the availability of satellite images have seen rapid advances in the 21st century. These new tools have become routine in monitoring land surfaces and environmental conditions and are nowadays essential in natural resource management (DeFries, 2013; Muhammad Aqeel Ashraf et al., 2010). Surface data captured by satellite sensors have become easily accessible products for users. They are routinely generated and provide spatially and temporally extensive sets of data. Multispectral images are data that contain information about the electromagnetic surface reflectance over several wavelength bands beyond the true–colour display that conventional photographs consist of. This study focuses on satellite platforms since these are readily available without having to conduct own surveys from the air. The information obtained by the most common remote sensing sensors can broadly be characterised through three main dimensions (DeFries, 2013):

1. The **temporal resolution** of a satellite in orbit is the revisit frequency of the satellite to a particular location. For example, the revisit frequency of every single Sentinel 2 (of which there are 2) satellite is 10 days, and the combined constellation revisit is 5 days.
2. The **spatial resolution** of an instrument is the *at−ground* representation of an individual detector in a satellite sensor array. It is often referred to as pixel size.
3. The **radiometric resolution** of an instrument is a determination of the incremental level of intensity or reflectance that can be represented or distinguished by the system (i.e. the brightness levels). Higher radiometric resolutions allow for the detection of finer differences in intensity or reflectance.

2.2.1 Satellite data pre-processing

User available data are made accessible at various levels of processing (Table 1). These range from the raw data as recorded by the sensor to fully processed and corrected imagery that requires the least user input. The higher the level of pre-processing, the less technical complex processing is required from the user. Therefore, this also makes the users dependent on the quality of these steps. The highest levels of pre-processed data usually relate less to surface reflectance information but rather geophysical parameters such as primary productivity or topography.

Table 1: The various processing levels at which data from remote sensing sensors is made user available

Level	Description
Raw data	The physical telemetry payload data as received from the satellite sensor.
0	Compressed raw image data. Reconstructed, unprocessed instrument data at full space−time resolution generally not made available to users.
1A	Same data as in level 0 but time−referenced and annotated with ancillary information, including radiometric and geometric calibration coefficients and geo−referencing parameters.
1B	Level 1A data radiometrically corrected and calibrated in physical units at full instrument resolution.
1C	Level 1B data orthorectified, resampled to a specified grid and most readily available to (public) users.
2	Derived geophysical parameters at the same resolution and location as Level 1 source data.
3	Data or retrieved geophysical parameters which have been spatially and/or temporally resampled (i.e. derived from Level 1 or 2 products), usually with some completeness and consistency. Such resampling may include averaging and compositing, resulting in generally smaller data and thus can be dealt with less data handling overhead.

In these processing levels, the data undergoes several correction steps to account for spectral distortions by physical phenomena, such as the atmosphere, the sun's azimuthal and positional errors (DeFries, 2013; Rumora et al., 2021). The energy that sensors record can differ from the actual energy reflected from the measured surface because of the properties of these physical phenomena.

The first correction is the sensor-specific radiometric calibration to convert the raw digital number to the radiance emitted from the top of the atmosphere (top-of-atmosphere or TOA). However, in most land and sea studies, the objective is to evaluate the surface reflectance or the bottom of atmosphere (BOA) radiance. Acquiring BOA radiance requires an atmospheric correction to remove the effects of scattering, absorption, and irradiance.

The ability to apply radiometric corrections differs across sensors due to the availability of parameters measured by the satellite's instruments, such a Landsat's and Sentinel's band 9 that are made explicitly for atmospheric water vapour estimates. Satellite data can undergo further corrections, such as correcting them for the effect of topography and aerosol. However, these are beyond the scope of this study and would make the techniques tested here unpractical to be applied to possible long-term monitoring procedures undertaken in the practical environment of nature conservation and planning.

2.2.2 Normalised Difference Vegetation Index (NDVI)

Over the last three decades, various VIs from satellite-derived data have been developed, each of them designed to be more suitable to describe certain biophysical properties of the land cover. For regions where the vegetation cover is sparse such as in the Arctic and Sub-

Arctic, including Iceland, researchers have been testing several VIs that are less sensitive to the optical properties of the soil background (Beamish et al., 2020; Eckert & Engesser, 2013). However, Eckert and Engesser (2013) reported no significant superior VI for measuring aboveground biomass and vegetation cover for the Satellite pour l'Observation de la Terre (SPOT) data in Iceland and therefore suggested that NDVI may be used for its convenience.

The usage of the NDVI in scientific literature is well established and has proven to be a remarkably successful tool for assessing aboveground phytomass (Myneni et al., 1995; Myneni & Williams, 1994; Pettorelli et al., 2005), especially in tundra ecosystems (Beamish et al., 2020; DeFries, 2013; Eckert & Engesser, 2013; Raynolds et al., 2015; Raynolds et al., 2012; Sundqvist et al., 2019).

Since the NDVI relies upon the surface reflectance of electromagnetic radiation, it is limited mainly by the presence of atmospheric particulates and vapour (e.g., clouds and aerosols). If conditions are so in the atmosphere that the reflectance cannot pierce through the atmosphere, or even if the reflectance is influenced by scattering, absorption or diffusion, the viability of the NDVI becomes negligible (Yengoh et al., 2016). However, correction measures such as previously described can, to a certain extent, counter the influence of atmospheric conditions. Further limitations to the NDVI are mostly reported on the complications of time–series analysis and other problems that are mostly related to other geo–physical properties not of concern to this study. Yengoh et al. (2016) reported that processing NDVI can be resource–intensive in the form of computing power, and scale variant, i.e. observing larger areas or in higher detail requires a greater investment of resources.

The NDVI, as developed by Rouse et al. (1974), is a standardised measure to assess the 'greenness' of vegetation which is an empirical approximation of photosynthetic activity (Asrar et al., 1984). It is measured as the difference between the amount of near-infrared (NIR) and visible red light (RED) reflectance, respectively, in the electromagnetic spectrum, normalised by the total reflectance of those wavelengths:

$$\text{NDVI} = \frac{NIR-RED}{NIR+RED}$$

NDVI values range from −1 to +1, where positive values indicate photosynthesis and negative values correspond to the absence of vegetation. The formula relies on the Chlorophyll cells absorption of RED, whereas the mesophyll leaf structure scatters NIR (Myneni et al., 1995). This makes this VI a well-suited measure of food availability for grazers which select for green leaf blades and feed most efficiently on grass swards with high green leaf biomass (Bro-Jørgensen et al., 2008).

Revegetation, restoration and protection from grazing have been the most common methods to rehabilitate vegetation cover and offset the ongoing soil erosion in Iceland. These measures and warmer summers were connected with an increase in vegetation productivity in Iceland during the 1980–2002 period (Raynolds et al., 2015). The greening trend had previously been identified over the tundra biome, from the coarser Advanced Very High Resolution Radiometer (AVHRR) data by Raynolds et al. (2012). In this earlier study, NDVI showed a remarkably strong correlation ($R2 = 0.94$, $p < 0.001$) with trans-Arctic field data of the total aboveground phytomass. Using the level 3 NDVI product from MODIS and the AVHRR satellites, Raynolds et al. (2015) suggested that these changes were driven by an

increase in mean annual temperatures and amplified by a reduction in sheep numbers and grazing pressures in the 1980s and early 1990s. The authors also reported a decrease in productivity for the period 2002−2010 using satellite-derived NDVI trends. This sudden decrease could not be confirmed using the NDVI, but it was suggested to be the result of non−biological processes such as ashfall and the construction of a hydropower reservoir.

2.2.3 Reindeer and Vegetation Indices

Ecological studies can use the diversity of spatial resolutions available from remote sensing images to answer a wide range of questions. Bro-Jørgensen et al. (2008) used the NDVI from three satellite sensors at four spatial resolutions to determine how different behavioural patterns by topi antelopes relate to resource abundance. Their findings illustrate how the spatial resolution of satellite-derived NDVI can affect the pattern of detection in ecological studies. With higher resolution, Bro-Jørgensen et al. (2008) could detect localised behavioural patterns which were invisible at lower resolution. In contrast, when forage was abundant, a positive correlation between the ungulate's density and NDVI was apparent at a lower resolution but larger scale.

Newton et al. (2014) identified a correlation with the Pen Islands caribou herd (*Rangifer tarandus ssp. caribou*) abundance and NDVI in the Canadian Low Arctic using Landsat 5 thematic mapper (TM). The relationship between caribou numbers was inversely correlated with NDVI, and growing degree days explained much of the variability in the NDVI. They concluded that the primary production in the area grazed by caribou was limited by them, with a time lag of six years in the NDVI signal. The index was a valuable tool for testing mechanisms of population change in herbivores, mainly where changes in forage occur across a broad spatiotemporal scale. In this way, the NDVI allowed for the investigation of land degradation as well as the movement patterns and density of the caribou herds.

Sundqvist et al. (2019) were unsuccessful in finding a relationship between reindeer densities and NDVI with hand-held sensors when studying the long-term effects of reindeer on Arctic vegetation greenness and species richness. However, NDVI was affected by reindeer when compared to reindeer excluded plots. It is suggested that this is due primarily to the NDVI being close to saturation (the value of 1) in more productive vegetation, and the reindeer's impact on the vegetation density was small there. In their study, the Leaf Area Index (LAI) was better at predicting the effect of changes in reindeer density and deciduous shrub cover (Sundqvist et al., 2019). Findings suggest that the LAI and NDVI have a scale-invariant relationship, although NDVI tends to saturate in areas of high vegetation productivity. Nevertheless, LAI remains a challenging indicator when measured with optical remote sensing unless accurate *in situ* measurements are readily available for validation (Beamish et al., 2020).

Rickbeil et al. (2015) applied the fraction of photosynthetically active radiation (fPAR) (i.e. a proxy of vegetation productivity derived from a combination of MODIS and AVHRR) to study grazing impacts of Barren ground caribou (*Rangifer tarandus ssp. groenlandicus*) and making use of the fact that fPAR is very closely related to the NDVI (Myneni & Williams, 1994; Yengoh et al., 2016). They found a negative relationship between fPAR and herd density between 1987 and 2013 in the western Canadian Low Arctic, further supporting the versatility of satellite-derived data for our understanding of ecosystems.

3 Material and methods

As described in the previous chapter, remote sensing methods are commonly used in tundra ecosystem research, including in Iceland. This provides the basis for the methods deployed in this study. The physical geography of Iceland and its tundra ecosystem is highly influenced by its northern location as well as its proximity to the Irminger Current and the mantle plume it lies upon (Arnalds, 2015). In this chapter, the region of this research in East Iceland is introduced and a case study area within this region defined. Additional data such as Boulanger-Lapointe's (unpublished) biomass data and the satellite data and their application for the remote sensing analysis are then described. Based on these data a grazing vulnerability index will then be developed.

3.1 The geography of East Iceland and Úthérað

Iceland is situated below the Arctic Circle, 66.6°N at its northernmost and 63°N to the south. It is considered to have a relatively mild climate for its northerly position due to the Irminger Current bringing warm waters in proximity to the shores acting as an external heat source (Arnalds, 2015; Einarsson, 1984). That is not to say that climatic conditions are favorable to vegetation productivity, mean temperatures are typically close to 0 °C in the winter and not far from 10°C in the summer. Ecosystems in Iceland are also greatly influenced by volcanic depositions, and anthropogenic modifications. It is an exemplary fragile northern ecosystem where these environmental properties have operated together resulting in severe land degradation (Arnalds, 2015, 2020; Eckert & Engesser, 2013).

The climate is maritime with cool summers and mild winters. Summers are short, and according to the Köppen classification, East Iceland is on the margin of the subarctic and polar zone (Björnsson et al., 2018; Einarsson, 1984). In 2019 at Egilsstaðir, the average temperature was 7.9 °C in June and 10.6 °C in July. July was wetter than June with total precipitation of 62.5 mm and 24.8 mm, respectively (Veðurstofa Íslands, 2019a, 2019b).

East Iceland varies greatly in vegetation cover, from well-vegetated highlands to deserts. Vegetation is in decline in the vicinity of highlands that have already undergone soil erosion to the extent of becoming deserts, but East Iceland is generally in good condition regarding grazing land. The rangelands are well vegetated and are among the best on the island when soil erosion is considered. However, the area is prone to severe precipitation in short bursts and steep hills characterise some areas. This results in vulnerable areas to erosion and previously vegetated slopes here have been replaced by scree in certain places. Soil sores on hillsides can undergo severe erosion very rapidly and are, therefore, particularly vulnerable to erosion (Arnalds et al., 2001).

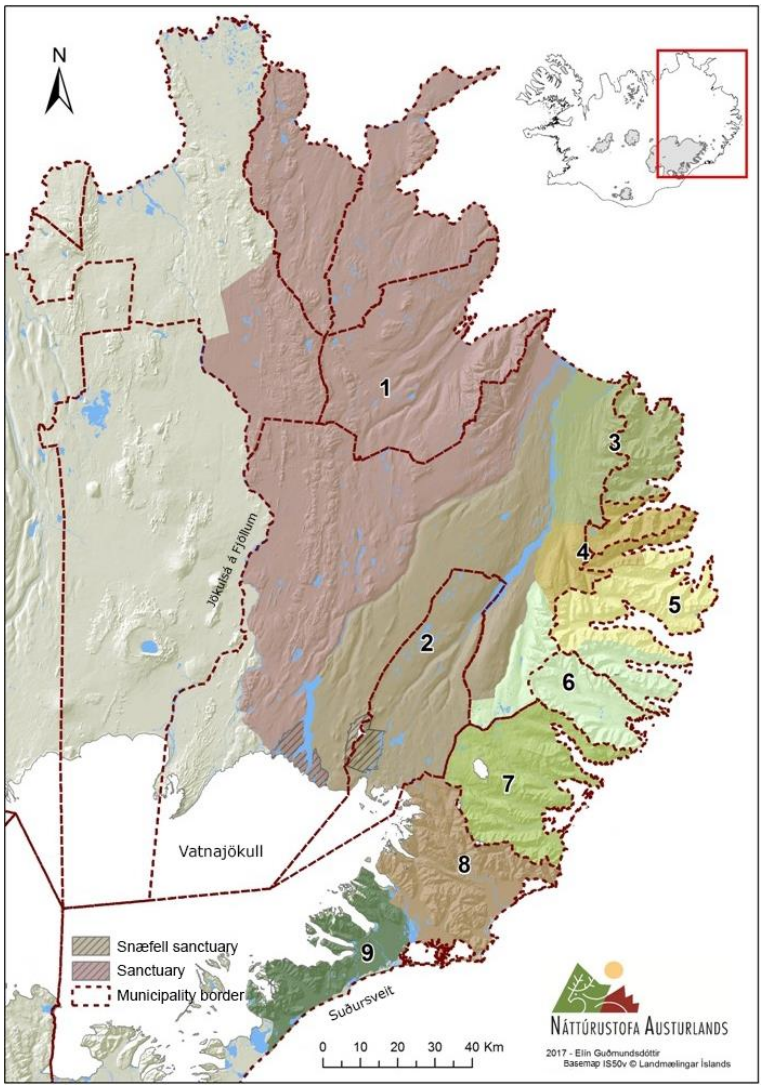

Figure 1: Reindeer hunting grounds in East Iceland.

Their hunting grounds are presented in different colors and numbered. Municipality borders have changed since this map was produced and has been modified from Guðmundsdóttir (2017).

The current distribution of reindeer is limited by Jökulsá á Fjöllum, Vatnajökull glacier and Suðursveit. Reindeer herds have been divided into nine hunting areas that are believed to reflect, to some extent, the local herd distribution (Figure 1). Here, Úthérað (65°34'39.5"N 14°18'03.1"W and 65°16'46.3"N 14°16'30.0"W) was selected as the sample area, specifically to the west of area 3. Heathland and moors predominate area 3 with some wetlands, but subalpine grasslands and barren areas are also typical at higher altitudes. The mountainous area to the east is changeable from steep hills with little vegetation to luxuriant valleys. Several farmed grasslands are situated within the selected area. These can be expected to be fertilised and cultivated, most likely resulting in some of the highest primary productivity.

3.2 Data acquisition

Different types of data were utilised in this study. This included biomass data related to the abundance of reindeer in the study area, and remote sensing data for the remote sensing analysis of the vegetation.

3.2.1 Biomass data

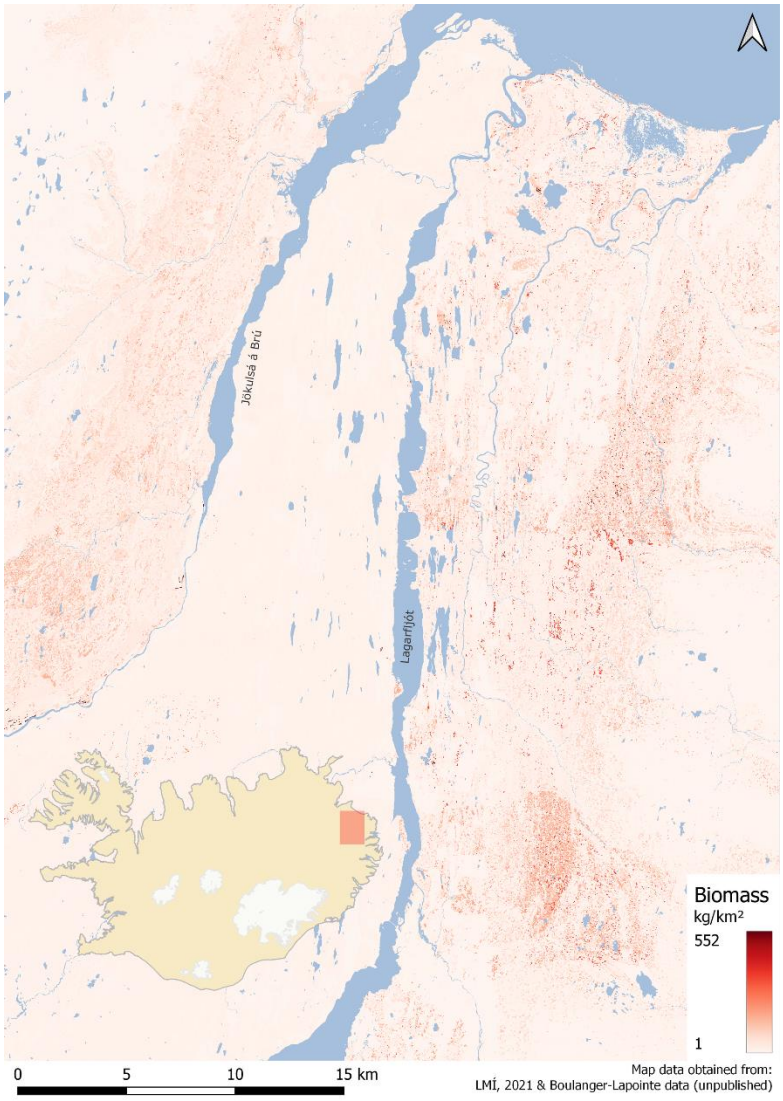

Figure 2: Reindeer's metabolic biomass map

The map was created from 2019 metabolic biomass data of reindeer per kilometre squared (Boulanger-Lapointe, unpublished data).

Reindeer grazing pressure was determined using the metabolic biomass of the species, which is an estimate of how much energy an individual consumes over the study area (Figure 2). The map was created as part of an ongoing project investigating the effects of wild herbivores on vegetation (Boulanger-Lapointe, unpublished). The map is based on raw census data collected by the East Iceland Nature Research Centre (Náttúrustofa Austurlands), namely the 2019 population census, reindeer biomass and GPS-collar data. The different data were combined using the Habitat Classification Map of Iceland (5 m resolution) for a resulting map presenting grazing pressure across the highlands in terms of the expected reindeer biomass (kg) per area (km^2). These kinds of species density rasters are relatively novel but have been previously used to determine terrestrial herbivore community structures and to link them to spatial patterns (Bubnicki et al., 2019).

The biomass raster has a very high spatial resolution, resulting in a large file size that assumes high precision of reindeer presence according to the habitat classification map. It relies on a high correlation between reindeer and habitat types, i.e. a strong habitat preference by the reindeer. On the map, a high concentration of reindeer biomass is visible on the east side of the river Lagarfljót and the west side of the river Jökulsá á Brú (Figure 2). Very little reindeer presence appears between the two rivers.

3.2.2 Satellite data

Free and publicly available data was selected to facilitate the establishment of a practical and affordable long-term monitoring procedure. With this objective in mind, four satellite sensors were selected from two different space programs; European Space Agency's (ESA) Copernicus program and the National Aeronautics and Space Administration's (NASA) EOS program. One high spatial resolution product and one high temporal resolution product with a multi-day composite were selected from each program (Table 2 and Table 3).

All satellite images used underwent radiometric, geometric and atmospheric correction prior to acquisition. Readily available level 3 NDVI products are accessible from the high temporal resolution satellites as the best available pixel value for a time period. The criteria for the selection of suitable data and geographic extent were (i) low cloud cover, (ii) low viewing angle, and (iii) the highest NDVI value. The highest NDVI value would represent the largest difference between the NIR and RED, defining the highest primary productivity, i.e. the most representative value for the aboveground phytomass.

Landsat 8 is a medium-resolution, multispectral imaging mission originally named the Landsat Data Continuity Mission (LDCM), but after operations were transferred from NASA to the United States Geological Survey (USGS) it was renamed Landsat 8 (*Landsat collection 2*, 2021). The spacecraft comprises of two cameras, the Thermal Infrared Sensor (TIRS) and the Operational Land Imager (OLI) of which most bands are consistent with the earlier Thematic Mapper (TM) and Enhanced Thematic Mapper Plus (ETM+) sensors from Landsat 5 and 7. Landsat 8 joins Landsat 7 on orbit for a more frequent revisit time, providing increased temporal resolution and coverage of Earth's surface. Two bands are needed for the NDVI, bands 4 and 5, each at 30 metre spatial resolution (Table 2). For a true colour image bands 2 and 3 are needed additionally (Figure 3). The portal to the user community is made by the Data Processing and Archive System (DPAS), which archives, calibrates, processes, and distributes all of Landsat 8 data and data products (U.S. Geological Survey, n. d.). DPAS radiometrically and geometrically corrects level 2 data that is made available to users.

Moderate Resolution Imaging Spectroradiometer (**MODIS**) constitutes identical payload imaging sensors onboard the Terra and Aqua satellites from the EOS program by NASA. The instrument captures data in 36 spectral bands with a relatively low spatial resolution of 250 metre to 1 kilometre, of which the MOD13Q1 v.6 level 3 products are generated (Didan, 2015). The highest pixel NDVI value is selected from a 16-day composite from the two different satellites with a MODIS-specific compositing method. The products complement the National Oceanic and Atmospheric Administration's (NOAA) AVHRR NDVI products, providing continuity for the time series applications of the archive. The NDVI product is computed from atmospherically corrected bi-directional surface reflectance that has been masked for water, clouds, heavy aerosols, and cloud shadows.

Sentinel 3 is a medium-resolution, multispectral imaging mission from the Copernicus Programme (ESA, n. d.). It makes use of multiple sensing instruments. The Sea and Land Surface Temperature Radiometer (SLSTR) and Ocean and Land Colour Instrument (OLCI) both take measurements in the visible and near-infrared spectrum. Sentinel 3 Synergy (SYN) products rely on the combination of SLSTR and OLCI instruments products as a continuity of SPOT's VEGETATION instrument. SYN products are derived from synergised and co-located measurements of OLCI and SLSTR. It provides a 10-day composite of the maximum NDVI value of ground reflectance measurements in 300 metre

spatial resolution called V10. Before applying the maximum NDVI selection, several rejection tests are applied on measurements quality, angle, cloud and cloud shadows, e.g. The product is then corrected for systematic errors and resampled to predefined geographic projections.

Sentinel 2 is a high-resolution, multispectral imaging mission, developed and operated by the ESA under the Copernicus programme (ESA, n. d.). The mission has two identical satellites (Sentinel 2A and Sentinel 2B) that operate together to achieve a more frequent revisit time and increase the temporal resolution as a result. The satellites each carry a single multispectral instrument (MSI) with 13 spectral bands. All data acquired by the MSI instrument are systematically processed by the Payload Data Ground Segment (PDGS) and made available to users as level 1C and level 2A products. The level 2A product provides geometrically and radiometrically corrected imagery of which two bands are needed to produce the NDVI, bands 4 and 8, each at 10 metre spatial resolution (Table 2).

3.2.3 Satellite data selection

This study was conducted using the Geographic Information System (GIS) software QGIS version 3.18 (QGIS Development Team, 2021) and the Semi−Automatic Classification Plugin (SCP) (Congedo, 2016) version 7.8.1 in a 64bit Windows 10 operation system environment. Computing resources available at the time of the study were a quad-core Intel i5-4670 processor at 3.40GHz with an 8 GB physical RAM.

The Earth Observation browser from the Copernicus program was used to explore images applicable to the study. SCP was used in QGIS to obtain the appropriate bands used to stack and create a multispectral image to calculate the NDVI (Congedo, 2016). The conditions used to capture optimal visibility as well as the height of productivity were: (i) low cloud cover (cloud cover values <8 %); (ii) acquisition date between 20. July and 10. August 2019; (iii) Low zenith solar angle. During this period, vegetation was assumed to have peak primary production in the area of interest, resulting in the strongest NDVI signal (Eckert & Engesser, 2013).

Table 2: Technical specification for Level 2 satellite data collected for this study

Satellite imagery metadata		
Satellite program	Sentinel 2	Landsat 8
Sensor	MSI	OLI
Acquisition date	Aug 02, 2019	Aug 03, 2019
Tile or Path/Row	T28WET T28WES T28WDT T27WXN	217/014
Data Level	2	2
Spatial resolution	10 metres	30 metres
Revisit time (temporal resolution)	5 days	8 days
Bands (nr)	RED (4)	RED (4)
	NIR (8)	NIR (5)
Bandwidth	RED: 646 – 685 nm	RED: 630 – 680 nm
	NIR: 767 – 908 nm	NIR: 845 – 885 nm

The pre-processed NDVI data from Sentinel 3 and MODIS were gathered using EarthExplorer from USGS (*Earth Explorer*, 2000). Data was selected based on the acquisition dates closest to the high spatial resolution images (Table 3). MODIS data are made available in hierarchical data format (HDF) without a projection. It is designed to store large amounts of data and includes several other bands and products aside from the NDVI. Similarly, Sentinel 3 is accessible as a Network Common Data Format (NetCDF or NC), serving the same purpose as the HDF, also without a geographic projection.

Table 3: Technical specification for the Level 3 satellite data collected for this study

Satellite imagery metadata		
Satellite program	Aqua & Terra	Sentinel 3
Sensor	MODIS	Synergy
Acquisition period	Jul 29, 2019– Aug 14, 2019	Jul 28, 2019– Aug 07, 2019
Tile or Path/Row	H17	North America
Data Level	3 v.006	3 VGK
Spatial resolution	250 metres	300 metres
Revisit time (temporal resolution)	1 day	<1 day
Bands (nr)	RED (1)	RED (8)
	NIR (2)	NIR (17)
Bandwidth	RED: 620 – 670 nm	RED: 660 – 670 nm
	NIR: 841 – 876 nm	NIR: 860 – 870 nm

3.3 Data analysis

The level 3 satellite data from the MODIS and SYN sensors were converted to GeoTiff files so that they were suitable for further analysis in a GIS environment. This also allows for the preservation of the original NDVI values throughout data processing steps. All data was projected in the WGS 84 Coordinate Reference System in QGIS for consistency and best compatibility with general satellite data formats.

The data collected varied in size, with the higher resolution images and the biomass being relatively large files. To facilitate the analyses, a sample area was put into focus where good images were available for the period of interest (Figure 3). This sample area was determined cloud−free on all images with a varying topographic landscape and a broad spectrum of reindeer biomass values. All images were clipped to the sample area for further analyses.

To analyse reindeer distribution in relation to primary production, the NDVI data had to be coupled with reindeer biomass cells through reprojection or resampling. The biomass raster, having the largest spatial resolution, was resampled down to the resolution of each satellite image. The resulting biomass raster could then be put in relation to the NDVI raster of the same resolution where each pixel matched in both sets of data. Resampling was conducted using bilinear resampling of the biomass data to each respective NDVI image's pixel size (*Technical Support*, 2020). Bilinear interpolation calculates the value of each pixel by averaging the values of the surrounding pixels. The method draws a weighted average from the four nearest cells of the biomass input raster, resulting in the output cell having a new value. This method was determined as the best representation of the pixels value since the assigned value is drawn proportionally from all surrounding pixel cells. The satellite image and the correlating biomass raster could then be merged into a multispectral image from which the NDVI−biomass index maps were made.

The raster pixels were converted to point vector data from the multispectral images. Points could then be joined on a polygon grid to extract the combined data as attribute tables. The resulting data table contains the NDVI and associated resampled biomass values for each feature (representing each individual grid cell in the original raster extent). Features with missing data values were removed before exporting the attributes. Extracted values were analysed and visualised using the statistical computing software R (R Core Team, 2017) and R package ggplot2 (Wickham, 2009). For the Sentinel 2 image, two outliers were excluded due to their unlikely high values (1872 kg/km^2) over such a small area. Removing these data did not affect averages or descriptive statistics but facilitated the visualisation of patterns.

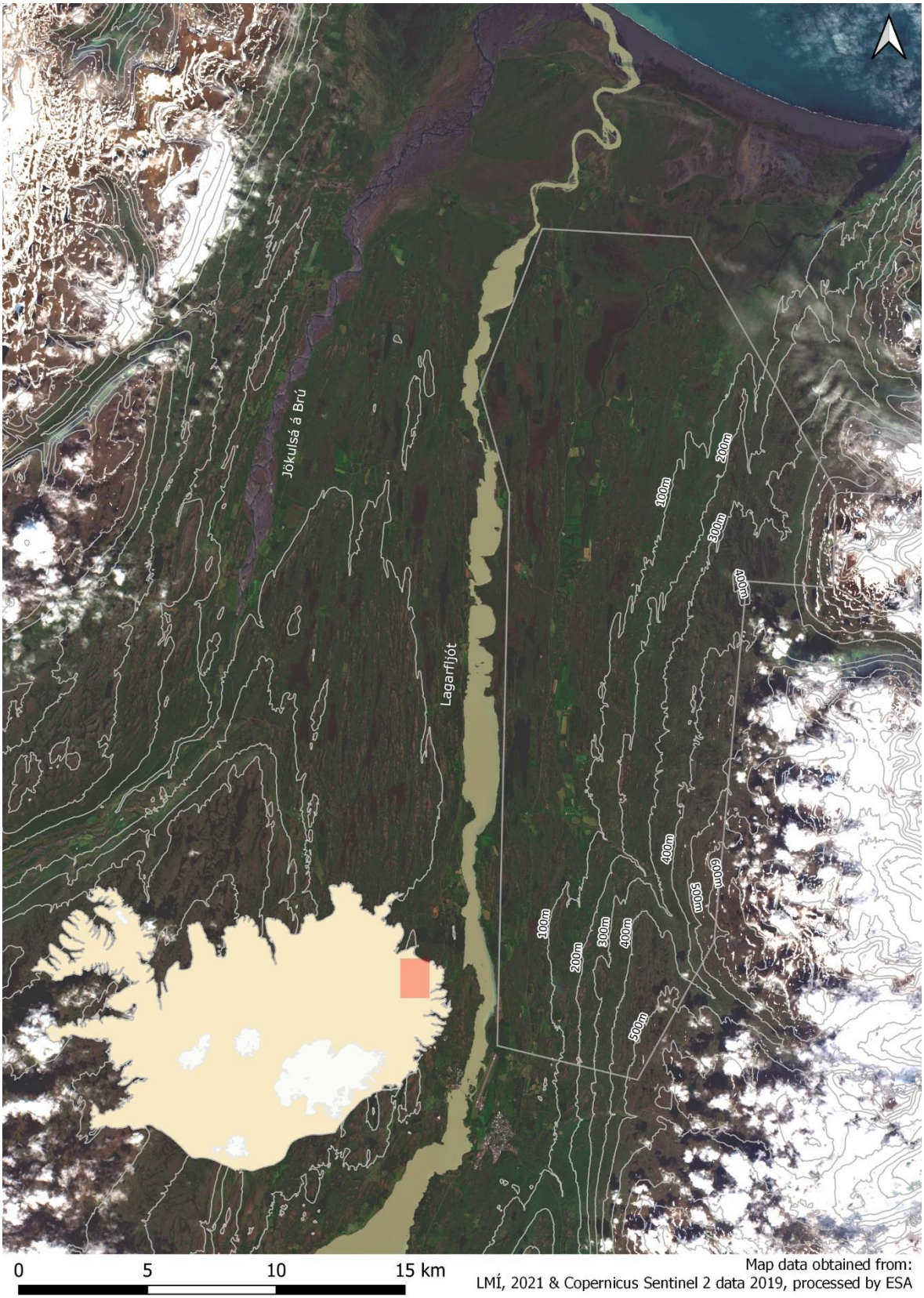

Figure 3: Overview map of the sample area in East Iceland.
100 metre contour lines with altitude show elevation within the sample area. Cloud–cover is visible in the east and some snow patches with increased elevation.

From the multispectral images the NDVI−biomass index maps could be created. Missing –data values, no vegetation values and the Sentinel 2 outliers were first removed from the multispectral images. Missing data values were removed to facilitate visualisation, while no vegetation values were removed since they hold no importance to primary productivity and phytomass. To remove the outliers, the following raster calculations were applied to the data:

$$"NDVIband >= 0" \times "NDVIband"$$

$$"Biomassband >= 0" \times "Biomassband"$$

The expression fetches all values above or equal to 0 and assigns them the value of one, which is then multiplied by its original value, leaving all other values as zeros. To create the NDVI–biomass index the NDVI, and biomass values had to be normalised by dividing them by their maximum value so that they could be reflected as a ratio:

$$\frac{NDVI/NDVI_{max}}{Biomass/Biomass_{max}}$$

The ratio can be interpreted in four quadrants, whereas the quadrant of importance to this study is the lower right one, with low productivity and high biomass i.e., high consumption (Figure 4). Should the primary productivity be high, abundant forage can be assumed, and should the biomass be low, it can be assumed that there is insignificant consumption or low grazing pressure. Thus, the values of concern are from 0 to 1 because relative consumption is higher than relative productivity, while all other values are 1 or higher. The ratio was then used as the index for maps from each satellite sensor. By excluding all other values from the maps, the index represents only vulnerable areas to grazing, and accordingly, it will hereafter be referred to as the grazing vulnerability index.

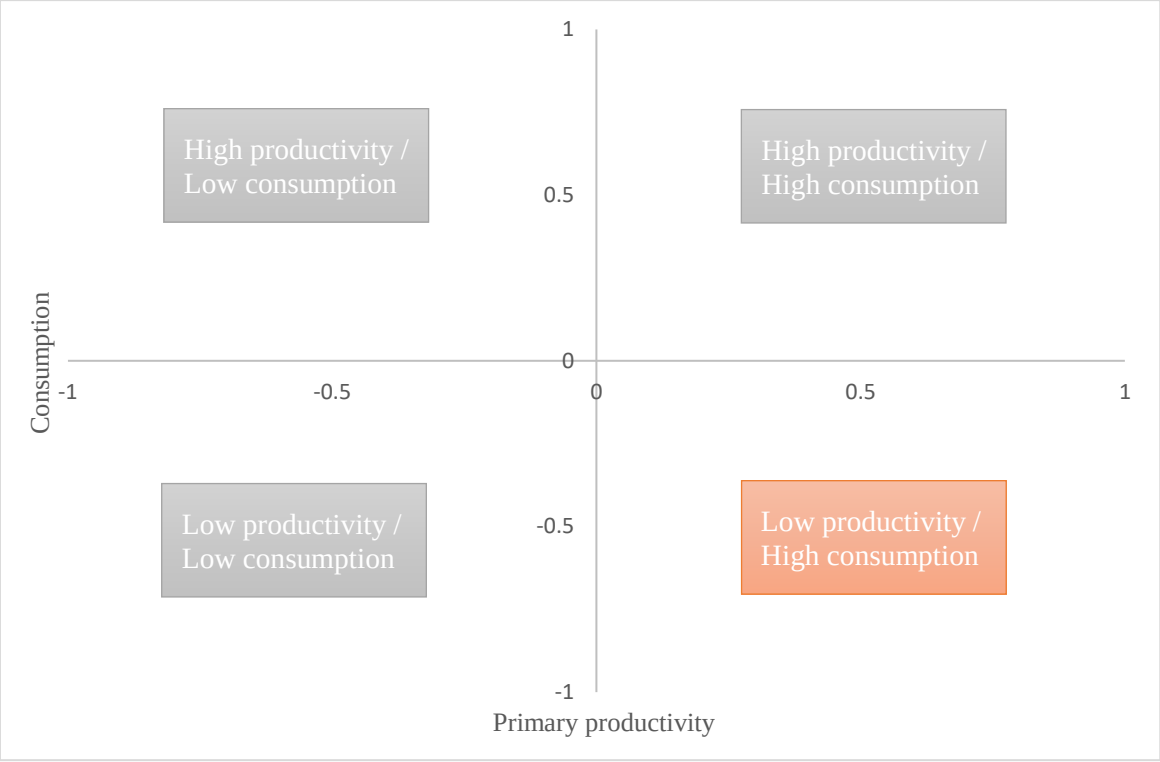

Figure 4: NDVI – biomass ratio quadrants presenting grazing vulnerability.

3.4 Conclusion

The aim was to create an index that could enable us to illustrate areas at risk of overgrazing by using biomass data and NDVI derived from satellite sensors. The first measures undertaken for the analysis were processing the data so that they resembled each other as practicably feasible. This was achieved by uniformising projections and resampling biomass data to the satellite images' spatial resolution. Due to the differences in spatial resolution, the analyses varied significantly in processing intensity. The high spatial resolution of Sentinel 2 and Landsat 8 images made the resampling procedure tediously protracted, while the processing of the level 3 data with high temporal resolution from MODIS and Sentinel 3 was very efficient.

Pixel values for both the NDVI and biomass were then normalised with their maximum value to calculate the ratio between primary productivity and consumption. This was an efficient procedure undertaken to correlate and juxtapose the two unrelated data sets—the presented forage availability and consumption, for and by reindeer. When the forage availability is low and the consumption is high, the vegetation is at risk of overgrazing by reindeer.

4 Results

Having outlined the procedure of creating a grazing vulnerability index using biomass and NDVI data, the results of applying it to a sample area will be described in the following chapter. The outcome of the data manipulation from the resampling and the differences in values between the satellites are presented. From there, the grazing vulnerability index maps are introduced and in details. Since this study was interested in testing the suitability of different satellite sensors to represent areas at risk of overgrazing by reindeer, the grazing vulnerability index maps are then analysed in term of their suitability for management.

4.1 Vegetation and reindeer

NDVI values obtained from the sample area of each satellite show some differences (Figure 4). MODIS had the highest average NDVI values, followed by Sentinel 2 and Landsat 8. Sentinel 3 showed the lowest average NDVI values. MODIS differed by 0.063 from Sentinel 2, while the difference between MODIS and Landsat 8 was 0.157, and Sentinel 3 was 0.249. Sentinel 2 had the highest measured NDVI value, closely followed by MODIS, differing by only 0.017. Landsat 8's maximum NDVI value was 0.07 lower than Sentinel 2, and Sentinel 3 had the lowest maximum NDVI value, 0.322 lower than Sentinel 2. Landsat 8 measured the lowest NDVI value, but the two Sentinel satellite sensors 2 and 3 had almost identical minimum NDVI values, 0.432 higher than Landsat 8. MODIS was the only satellite with no NDVI value below zero with a minimum NDVI value 0.701 higher than Landsat 8's lowest value.

Table 4: Average, maximum and minimum NDVI values from all four satellite sensors

Satellite sensor	Average [NDVI]	Maximum [NDVI]	Minimum [NDVI]
Sentinel 2	0.674	0.938	-0.228
Landsat 8	0.580	0.868	-0.660
Sentinel 3	0.488	0.616	-0.228
MODIS	0.737	0.921	0.041

Histograms created from pixel values of the NDVI from each satellite sensor, respectively, are all left–skewed with similar medians and means (Figure 5). Sentinel 2's histogram has a gradual rise to its mode while Landsat 8 presents lower NDVI values. Sentinel 2 and Landsat 8 have several columns with similar quantity of NDVI values across a broad range. MODIS appears to have almost only two columns of relatively high NDVI values, and similarly, Sentinel 3 has almost all its NDVI values within one column although with much lower values.

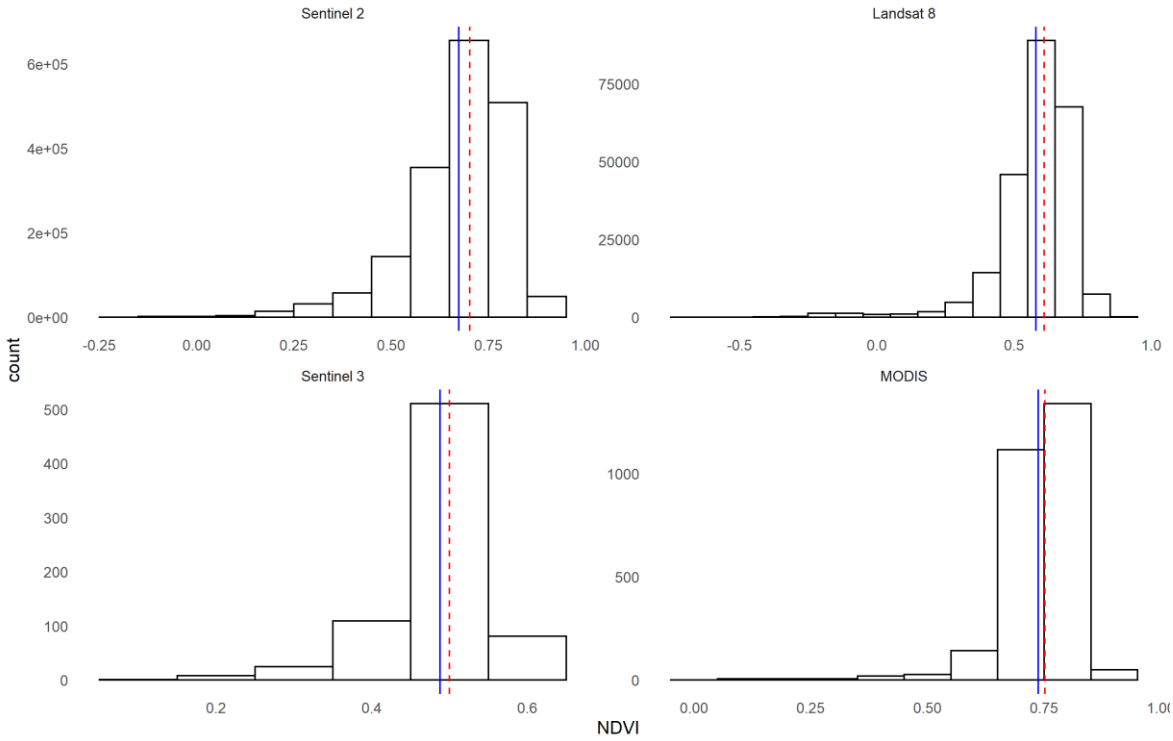

Figure 5: Histograms of NDVI value quantity from each satellite sensor used.
The median is shown as a dashed red line and the mean is a blue lines on the histograms.

Since the biomass raster had to be resampled to the same spatial resolution as the satellite sensors to create the grazing vulnerability index, the range of biomass values also changed from one map to the other. The bilinear resampling of the unprocessed raster of metabolic biomass created new biomass values. Each satellite, therefore, got assigned biomass values from the resampling measure that differentiated between them (Table 5 and Figure 6). The output cell corresponds to the satellites larger pixel size but draws its values from the biomass raster.

The average biomass values were almost the same as the original raster for the resampled biomass raster at the spatial resolution of Sentinel 2, Landsat 8 and Sentinel 3 (Table 5). MODIS had only a slightly lower average, by 1.16 kg/km^2 than the original raster. The maximum and minimum biomass values for the satellites varied with spatial resolution. Sentinel 2 had the highest value, followed by Landsat 8 with 79.12 kg/km^2 lower maximum. MODIS and Sentinel 3 had lower maximum values by 324.51 and 329.21 kg/km^2 and showed a similar data distribution. Sentinel 2 and Landsat 8 had the same minimum biomass value as the original biomass raster, while the minimum biomass values for Sentinel 3 and MODIS were higher by 0.04 and 0.91 kg/km^2, respectively.

Table 5 Average, maximum and minimum biomass values after resampling to each satellite sensors pixel size and the original biomass raster.:

Corresponding raster	Average [kg/km^2]	Maximum [kg/km^2]	Minimum [kg/km^2]
Sentinel 2	21.10	413.06	0.07
Landsat 8	21.10	333.94	0.07
Sentinel 3	21.18	83.85	0.11
MODIS	19.94	88.55	0.98
Metabolic biomass	21.10	1,832	0.07

The resampled biomass values histograms, with their corresponding satellite sensors spatial resolution, are right–skewed and have similar modes (Figure 6). Minimum and maximum values range from 0.07 to 1832 kg/km^2 in the original biomass raster and this range decreases with spatial resolution. The resampled biomass histograms mode values are on the lower side or around 20 kg/km^2. The histograms for the high spatial resolution images have notably more biomass values than the high temporal resolution images since their pixel size is smaller but the sample area is identical.

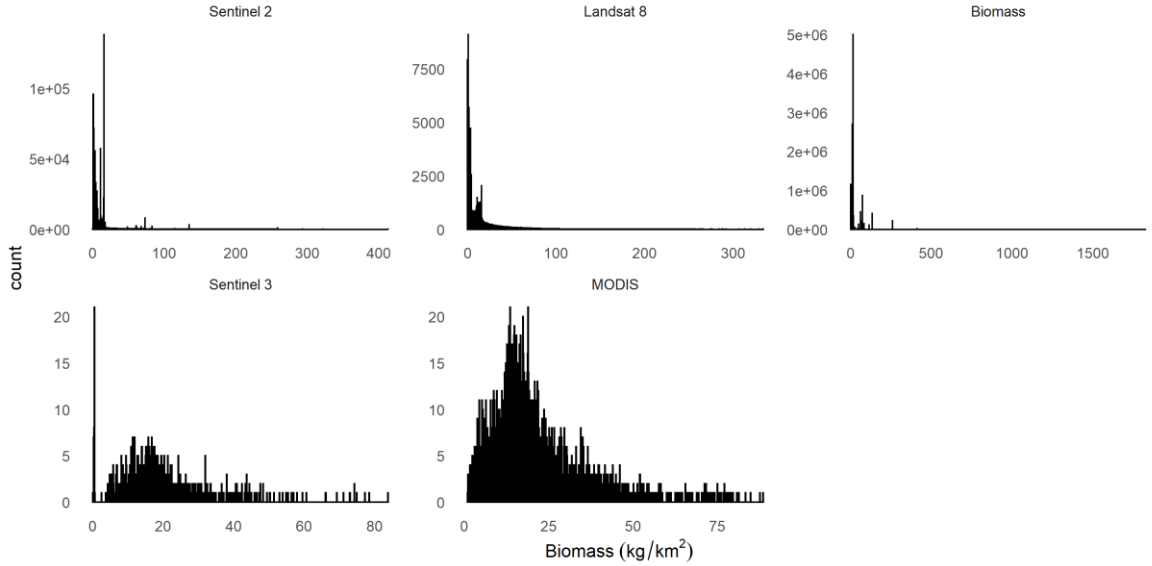

Figure 6: Histograms of biomass value quantity.
Each satellite sensor got assigned new values after resampling the biomass to the satellites' spatial resolution. The histogram of the original biomass raster is also shown.

The scatter plots show the relationship between the NDVI and biomass pixel values in the stacked raster image (Figure 7). The biomass values (in kg/km^2) are shown on the y–axis and NDVI on the x–axis. The higher spatial resolution images, Sentinel 2 and Landsat 8, scatter plots resemble a left–skewed standard distribution curve while the high temporal images appear more irregular. The high temporal resolution satellites do show a concentration of high NDVI values. The concentration appears mainly around the same values of NDVI as the highest measured biomass values are found. The difference in pixel quantity is also apparent on the scatterplots. The higher spatial resolution satellites have much more pixels and more points on the plots, thus their plots are more concentrated with data points than the lower spatial resolution satellites.

In the scatterplot for the Sentinel 2 data and associated biomass, the original biomass categorisation is visible due to its high spatial resolution and the resampling method used for the biomass raster (Figure 7). Since biomass values were assigned to the habitat classes, their distribution was not continuous. For this reason, the raw biomass values have visible intervals. This is apparent on the scatterplot as four lines of accumulated data points, with the same, or very similar, biomass values, form with a range of NDVI values, parallel to the x-axis. These grouped values disappeared in the lower spatial resolution rasters due to the resampling procedure.

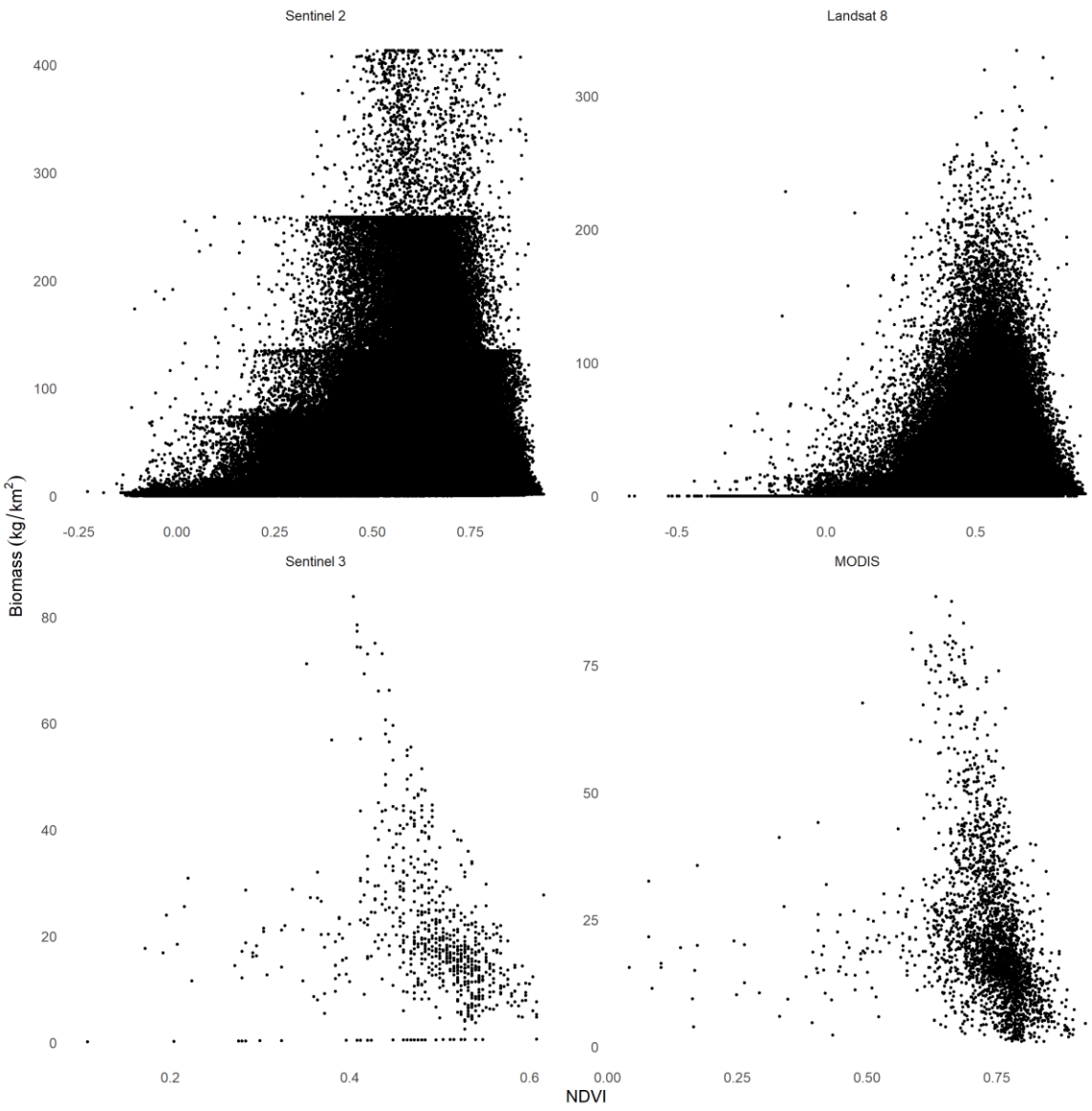

Figure 7: Scatter plots of biomass and NDVI for each satellite sensor, respectively.

4.2 Grazing vulnerability maps

The grazing vulnerability index highlights low productivity and high reindeer abundance areas (Figures 8 to 11). Four maps have been created using the grazing vulnerability index with pixels that fall under the lower right quadrant of the grazing vulnerability index (Figure 4), highlighted with a red gradient colour, darker red signifying increasing vulnerability. All the maps show similar patterns, with areas in two corners of the map by the east side of the sample area, under risk of overgrazing by reindeer (Figure 8). The middle of the sample area does not show any prominent vulnerable areas, nor does the western side of the sample area.

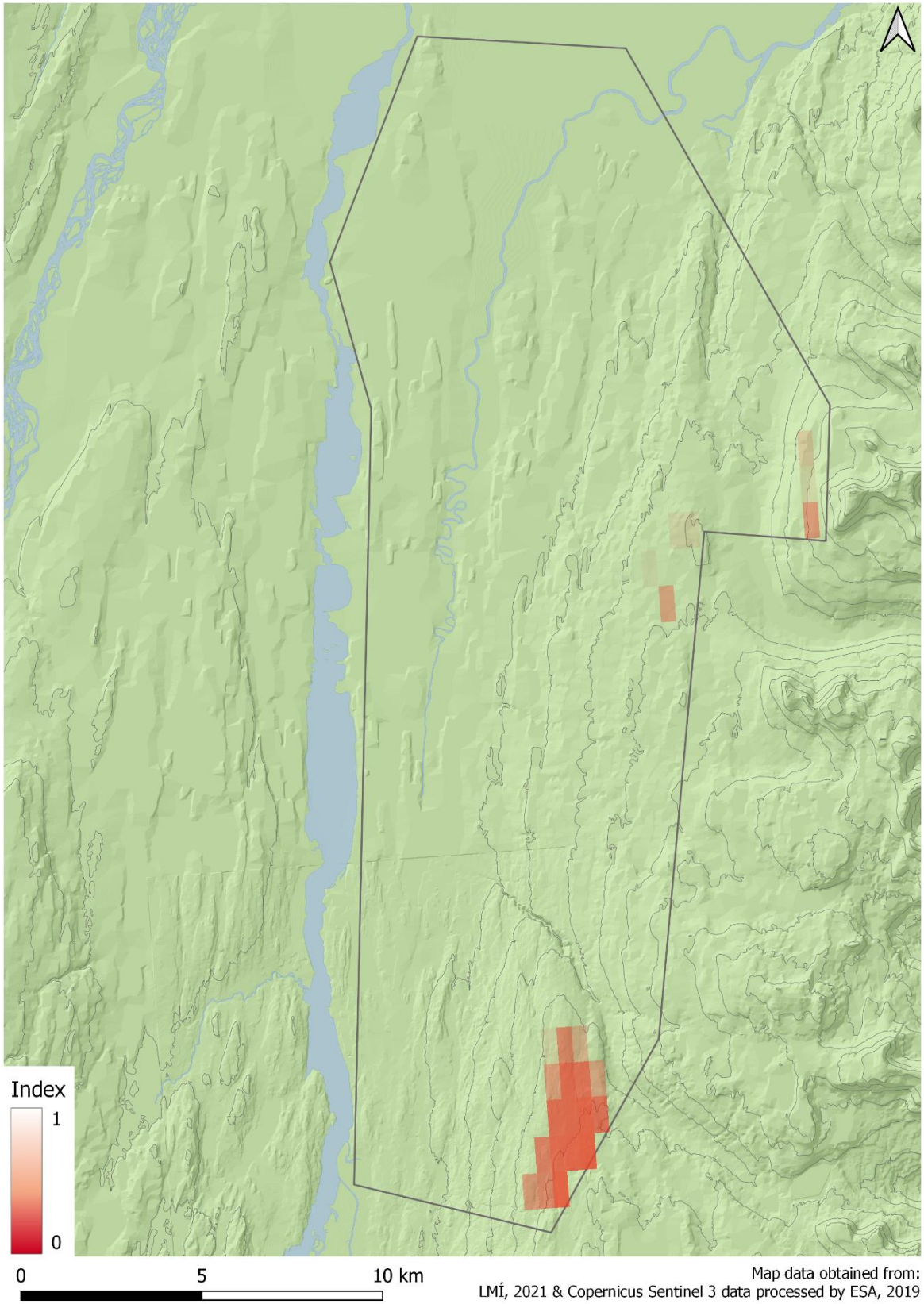

Figure 8: The grazing vulnerability index generated with Sentinel 3's sensor.

Map of the sample area, in Úthérað, showing the grazing vulnerability index generated with Sentinel 3's SYN V10 NDVI composite and reindeer biomass data.

On the high temporal resolution satellite images, the low spatial resolution is evident. The pixels, indicating vulnerability, are much larger and covers larger areas. Similar patterns are evident with maps from satellites at similar spatial resolution, especially on the lower spatial resolution satellites' index maps, where the eastern side of the sample area shows a vulnerable area. The areas highlighted by the grazing vulnerability index are relatively large patches on the north- and south-eastern boundary of the sample area. The Sentinel 3 map (Figure 8) displays high grazing vulnerability pixels almost exclusively on the southeast corner, with only a few pixels in the northeast corner. No pixels fall under the vulnerable category on the middle or western side of the map. The MODIS map (Figure 9) has a few highlighted pixels in the north–eastern corner but similarly, the concentrated red area is in the south-eastern corner of the map and a few, mostly diluted, pixels scattered around the eastern border of the map.

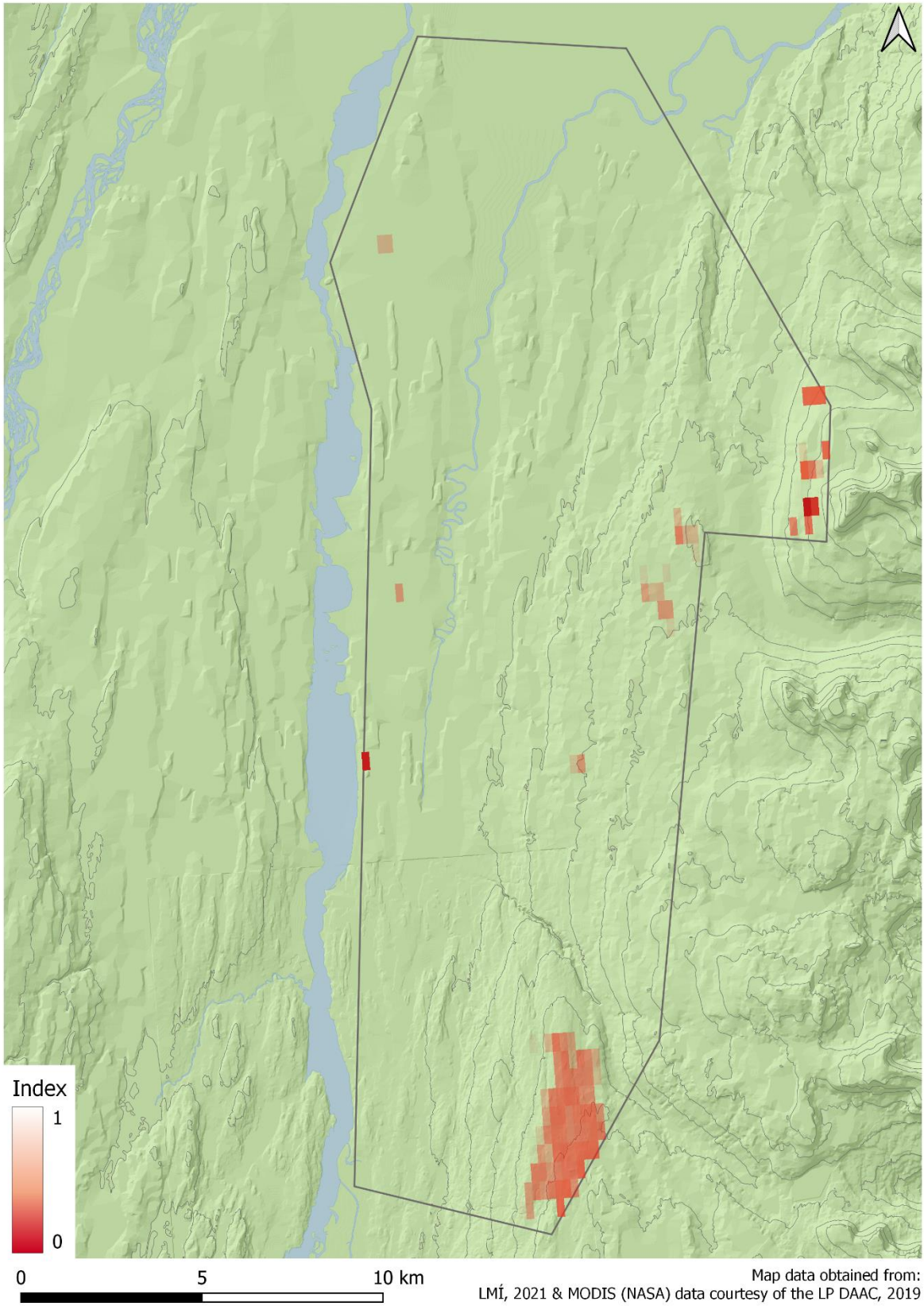

Figure 9: The grazing vulnerability index generated with MODIS' sensor.
Map of the sample area, in Úthérað, showing the grazing vulnerability index generated with MODIS' MOD13Q1 NDVI composite and reindeer biomass data.

The clusters of high grazing vulnerability pixels are less visible on the high spatial resolution images, but when the patches are enlarged, they appear smaller and more dispersed. On the Landsat 8 map, there is an apparent aggregation of pixels indicating vulnerability to grazing in the east of the sample area (Figure 10). These are the most evident in the same areas as were highlighted by the high temporal resolution maps (Figure 8 and Figure 9). The Sentinel 2 shows the same trend, with a concentration of high vulnerability pixels in the two eastern corners of the map (Figure 11).

On the higher spatial resolution maps, aggregation patterns are more difficult to perceive due to their smaller size. They are dispersed over the same region between the different resolutions, although appearing less concentrated with higher spatial resolution or smaller pixel size. In contrast, the high spatial resolution maps display an aggregation of several vulnerable areas on the western side of the sample area. A few red pixels are scattered around the western side on the lower resolution images, but they do not show concentrated areas as apparent on the eastern side. On these high spatial resolution maps, smaller patches of vulnerable areas are scattered around the whole sample area (Figure 10 and Figure 11). Although not clearly visible, some patches can be found to the northwest on the sample area and by the middle of it. These are, however, not as evident on the high temporal resolution maps (Figure 8 and Figure 9).

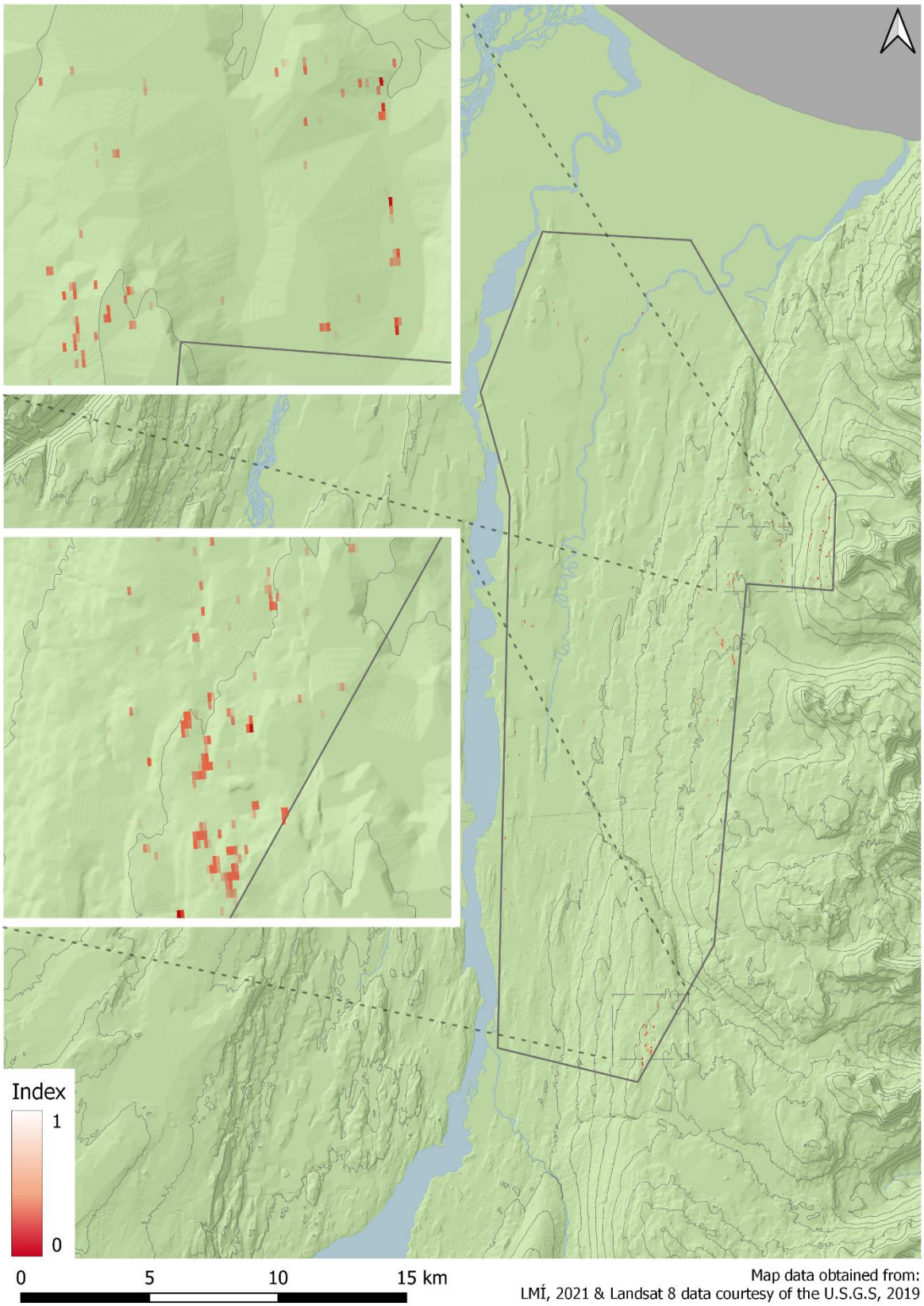

Figure 10: The grazing vulnerability index generated with Landsat 8's sensor.

Map of the sample area, in Úthérað, showing the grazing vulnerability index generated with Landsat 8's RED and NIR bands and reindeer biomass data.

4.3 Satellite compatibility

Because high spatial resolution data was not publicly available as a level 3 pre-processed NDVI product, the RED and NIR bands of Sentinel 2 and Landsat 8 had to be manually collected, combined, and processed into an NDVI map. The NDVI was therefore obtained and generated manually which required high processing capacity and significant data manipulation. With a larger sample area, these steps would have been beyond the computational capacity available to this study.

Finding appropriate Sentinel 2 and Landsat 8 images was problematic due to the frequent cloud–cover days and the high revisit time of both satellites. The sample area used here was limited by the cloud–free images available from both satellites since those were the only images available during the predefined period in that year. The tiles obtained from Sentinel 2 were also small, so four tiles had to be compiled to generate a map of the whole sample area, adding to the processing steps for this satellite.

The Level 3 data from the MODIS and Sentinel 3 satellites had readily available NDVI products that were publicly accessible. It was generated from satellites with a more frequent revisit time, thus having higher temporal resolution. The tiles cover extensive areas larger than Iceland as a whole and come with multiple layers of related data, such as the bands used for calculating the NDVI and a pixel reliability index. Their low spatial resolution made the file sizes smaller, requiring less processing capacity, however, obscuring more detailed features. With the multi–day composite factors such as: cloud cover, geometric viewing conditions (view zenith and azimuth, sun zenith and azimuth), became less of a concern. This gives the level 3 data advantages in Iceland due to the risk of cloud cover and shadows.

The high spatial resolution resulted in smaller areas highlighted by the grazing vulnerability index maps than with the high temporal resolution images. Relatively vulnerable areas became obscured in the surrounding patterns since most of the pixels from the index fall into one of the grazing vulnerability index quadrants (Figure 4) that are unlikely to be at risk of overgrazing. For this reason, vulnerable areas are difficult to identify on the high spatial resolution maps unless already identified and enlarged. However, the vulnerable areas are expected to be geographically more accurate than on the high temporal resolution images.

Landsat 8, MODIS and Sentinel 3 have a history of satellite sensors acquiring comparable data products complementing more recently obtained data. Landsat 8 sensors TM and ETM+ are like Landsat's 4, 5 and 7 that have been orbiting Earth since 1982, however not providing vegetation monitoring or an NDVI specific product. MODIS' NDVI product is an extension of NOAA's vegetation monitoring program utilising the AVHRR instrument which has been in orbit since 1998. Similarly, SYN from Sentinel 3 is a continuity of VEGETATION from the SPOT program launched in 1998. Thus, these satellites have a historical data record that is compatible with their more recently acquired images, making them advantageous for long term spatio-temporal research.

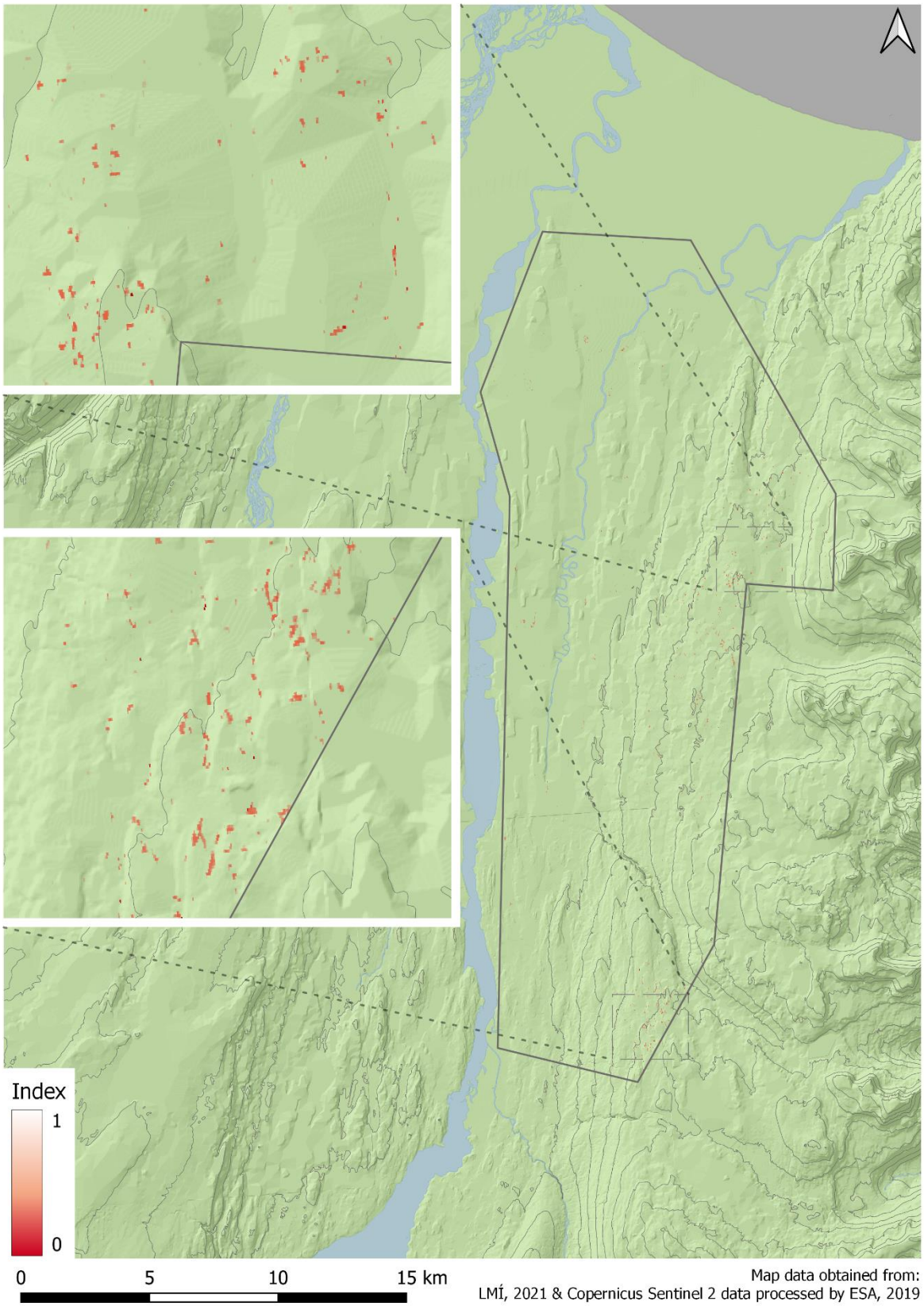

Figure 11: The grazing vulnerability index generated with Sentinel 2's sensor. Map of the sample area, in Úthérað, showing the grazing vulnerability index generated with Sentinel 2's RED and NIR bands and reindeer biomass data.

4.4 Conclusion

Data analysis and processing varied depending on the type of data, i.e. the file format and spatial resolution. The high temporal resolution data required adjustment in the file format and the biomass data had to be resampled to a significantly different spatial resolution. This resulted in the highest biomass values dissolving in the average surrounding patterns on the high temporal resolution images. The details of maximum values are more evident in the high spatial resolution biomass rasters. The scatter plots show a difference in satellites and a normalised curve in the high spatial resolution.

The NDVI–biomass ratio was used to create grazing vulnerability index maps that show patterns of areas at the risk of overgrazing. These areas were portrayed on maps for all satellite sensors and showed similar regions at risk between them. The high temporal resolution satellite maps had more obviously visible regions highlighted while the high spatial resolution satellite maps picked up vulnerable areas in more details, resulting in some areas only categorised as vulnerable in the high spatial resolution.

The resolution of the different satellite sensors makes the data suitable to answer a wide range of ecological questions. The high spatial resolution satellites can give us insights into detailed patterns that are not evident on the high temporal resolution satellites. The high temporal resolution images are more reliable since they use multi-day composites. They are also less resource-intensive regarding computing capacities for processing them. Therefore, they can be used in much greater study areas with less computational capacity at hand, which makes such procedures suitable to be used in a practical planning environment rather than a specialised engineering environment. Furthermore, the high temporal resolution is more reliable, especially for remote sensing research conducted in Iceland due to the frequent cloud cover and changing solar azimuth following seasonal changes. Both satellite categories, high spatial and temporal resolution, respectively, have their benefits and disadvantages and must be compatible with the study site size (Table 6).

Table 6: Advantages, issues, and best fits of several satellite–derived NDVI products.

Satellite	Description	
Sentinel 2	Advantages	Clear and detailed images due to high spatial resolution. 2 satellites equipped with identical sensors results in higher temporal resolution. Easily visualised prior to gathering
	Issues	Resource intensive due to large files and multiple tiles. Important patterns can be hidden in the high the detail.
	Best fit	Micro−Meso sized study area.
Landsat 8	Advantages	High spatial resolution. Long series of similar satellites from the same provider (Landsat). Displays correlation with biomass data. Larger tiles relative to S2
	Issues	Resource intensive due to large files. Low temporal resolution.
	Best fit	Mesoscale area of interest.
Modis and Sentinel 3	Advantages	Best pixel value out of a 16-day acquisition composite. Readily available NDVI. High temporal resolution (2 sensors with 1−2 day global coverage)
	Issues	Low resolution makes details vanish in pixels average. Granular images of sample areas.
	Best fit	Meso−Macro study area. Large spatio-temporal scale research.

5 Discussion

In the previous chapter, the differences in satellite sensors compatibility for the use of grazing vulnerability research have been reviewed and a grazing vulnerability index was introduced to create maps highlighting areas at risk of overgrazing for each satellite. In this chapter, these results will be discussed in relation to satellite suitability for this method. The grazing vulnerability index will then be reviewed, considering what is known about the sample area and established knowledge of vulnerable areas to overgrazing.

5.1 Satellite suitability

In this research, I intended to assess the applicability of different, publicly available sensors to detect vegetation signal in relation to reindeer with the NDVI. Differences in maximum and minimum values for the resampled biomass values were evident but also for the NDVI Figure 4 and Table 5). The histograms and scatter plot showed the same differences as well as differences in the distribution of values (Figure 5 – Figure 7). Although the satellite images represent in theory the same conditions in the field (i.e., taken from the same area at the same time), different NDVI scales are noticeable, highlighting differences between sensors. Since acquisition dates are very close in time, real differences in primary productivity are unlikely and the differences observed are linked to acquisition techniques.

These differences can be attributed to the spatial resolution of each sensor and the multi–day composites of the high temporal resolution satellites. Details in the high spatial resolution images are more apparent, resulting in more intensive maximum and minimum NDVI values that the surrounding values would otherwise average out. Lower NDVI values present insignificant primary productivity or minimal forage for reindeer. Since the NDVI is used as a vital component of the grazing vulnerability index, pixels with extreme NDVI values relate to the index's extreme values. This could be useful in spatiotemporal research to investigate whether these extreme pixels increase or decrease in numbers or are coalescing. This is a well-established method used when analysing NDVI alone (Raynolds et al., 2015). However, the metabolic biomass data allows us to monitor it in relation to reindeer presence by utilising the grazing vulnerability index.

By applying the method described in this paper over several years, the frequency of extreme grazing vulnerability index values can be monitored, giving us insights into whether areas at risk would be increasing in size or intensity. The advantage of the high detail is in observing these patches as they develop instead of seeing them as part of an averaged value in a much larger pixel. We can then detect areas at risk much sooner than otherwise since they become apparent as a pixel in the grazing vulnerability index.

The high temporal resolution images have a multi-day composite where one of the criteria for choosing pixels is the highest NDVI value during image acquisition. NDVI values are expected to be higher accordingly, and extreme minimums are less likely. This was not the case for Sentinel 3 in this study (Figure 4). Sentinel 3 had the lowest NDVI mean, and maximum value and a low minimum value relative to the rest. It might be an accidental

occurrence due to cloud–cover during the 10-day acquisition period (MODIS has a 16-day acquisition period) or the low spatial resolution averaging the extreme values. Whether that is the case here is beyond the scope of this study and requires further investigation.

NDVI values should generally be higher in the high temporal resolution images with composites due to the highest NDVI values being selected. In the high temporal resolution images, details are compromised, making them less suitable for observations of smaller plots and observing detailed patterns. More general patterns are instead revealed and more noticeable (Figure 12). For monitoring the entire reindeer habitats, these enhanced patterns highlight areas at risk of overgrazing more generally. Similarly, as with the high spatial resolution images, the high temporal resolution images can allow us to detect changes over time by utilising the grazing vulnerability index. This could be done by observing the evolution in the index over time in a specific area. This method would allow the detection of changing ratios between forage and grazing pressure, and should the index values decrease, less forage will be available for reindeer. Since the high temporal data is in low spatial resolution, the pixel covers extensive areas, but the grazing vulnerability index gives us a good idea of whether the area is likelier at risk or not.

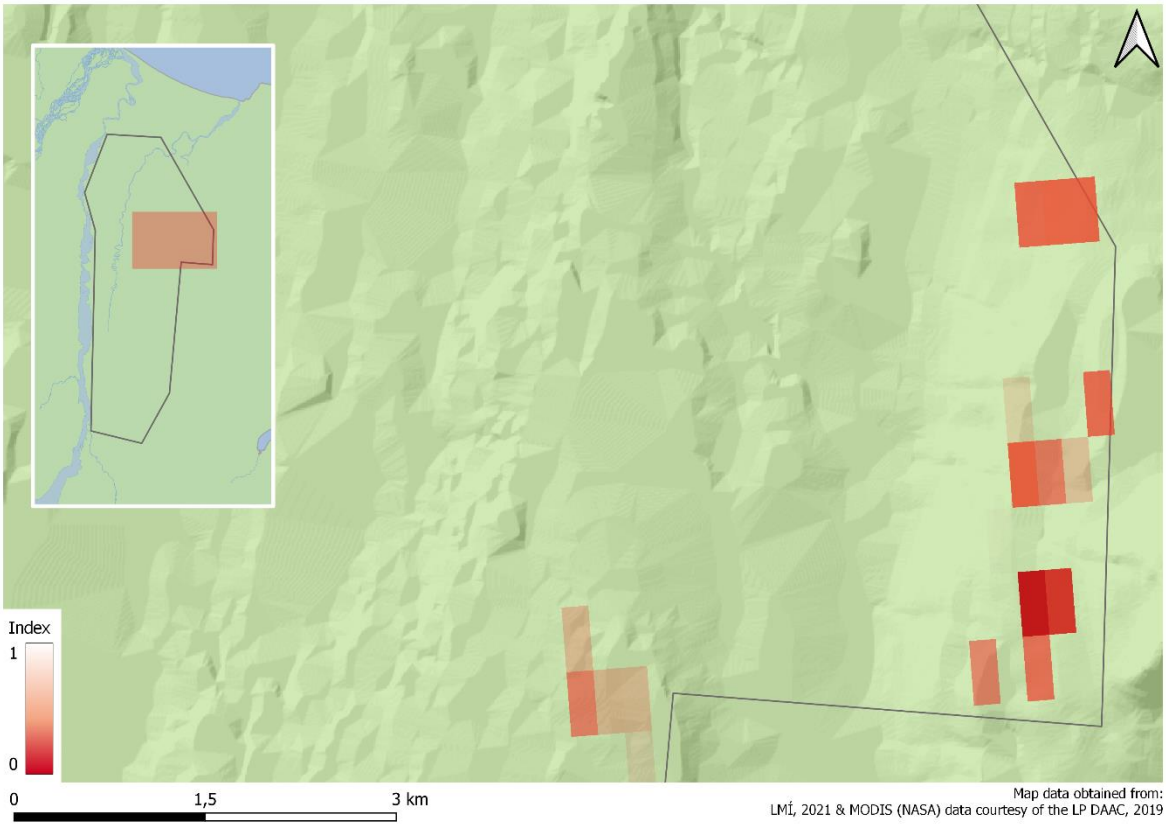

Figure 12: General grazing vulnerability patterns observed with MODIS's low spatial resolution

Another leverage of the high temporal resolution data is embedded in the frequent and extensive cloud coverage in Iceland. This makes appropriate data availability one of the main limiting factors for remote sensing methods. Here, temporal resolution can play a major role in obtaining data, with composing products, such as the MOD13Q1 and SYN used in this research. Images from two or more satellites are then combined into a single product making it an even more effective device, since the satellites revisit time is different. Cloud cover is often patchy so good quality pixels can be obtained; in secluded areas, during an acquisition period and then joined together into a full image of the region, with only the

most appropriate pixels. These images are likely best for representing the surface reflectance and are, therefore, generally more reliable.

The high temporal resolution imagery has a lower spatial resolution, making the data smaller and requiring less computational capacity. Making composites with smaller file sizes is less resource–intensive compared to high spatial resolution images so that it could be more easily embedded in other workflows and in a practical non-specialist environment. It is more time and resource intensive to detect detailed patterns. Detailed analyses could be useful to answer some ecological questions but may not always be required to obtain good results.

Possible NDVI value preferences

On the scatter plots the distribution curves show significant differences (Figure 7). The biomass values and NDVI, have different distributions between all satellite images, although they are from similar observations. The scatter plots from the high spatial resolution images show a curve resembling a normalised distribution while the plots from the high temporal resolution images appear more irregular. Thus, a difference between the satellite images when measuring NDVI and the correlating resampled biomass values (Figure 5 and Figure 6). Some of the differences can be associated with the resampling procedure for the biomass raster, however, whether a normalised distribution curve will become apparent with the high temporal resolution images with a larger sample area is a question that needs to be addressed in further analyses.

Furthermore, the distribution curve might suggest an NDVI preference by the reindeer. The highest biomass values are apparent within an NDVI spectrum indicating an attraction to a certain NDVI signal. This would resemble Bro-Jørgensen et al. (2008) findings of certain behavioural patterns detectable by an NDVI signal during specific seasons. The ungulates they studied preferred areas with a certain NDVI signal prior to, and during the rut, respectively. Similarly, a certain NDVI spectrum might represent areas of reindeer's prefered forage grounds. However, certain limitations within this study and its data are present, barring these assumptions. Notably. the biomass data from Boulanger-Lapointe (unpublished) was generated using the habitat classification map of Iceland. The habitat classification map is likely generated by an NDVI-like product which would translate to the reindeer biomass map. Whether that is the case here is beyond this study and requires further analyses into (i) the link between the habitat classification map and an NDVI-like product, (ii) to what degree does that translate into the biomass data (iii) and is there a statistical correlation between the reindeer's metabolic biomass data and the NDVI signal.

5.2 Grazing vulnerability index

One of the objectives of this study was to present an index evaluating the vulnerability of the vegetation in East Iceland to reindeer grazing, several maps were produced using a grazing vulnerability index (Figure 8 to Figure 11). The index generated as part of this research is greatly influenced by each measure, NDVI and biomass, respectively. Satellite-derived NDVI data were obtained and made relatable to biomass data of reindeer presence. The maps created from this approach present values with high consumption and low productivity pixels, thus highlighting areas vulnerable to grazing. As has been suggested by Bernes et al. (2015), the reindeer's grazing pressures are less likely to affect productive areas and therefore, the focus here has been set on areas with low productivity.

Spatial analyses allow us to put spatially connected measures in relation to one another. In this study, the grazing vulnerability index gives an indication of where overgrazing may be occurring, as registered by values between 0 and 1. It is important to see these as hypothetical observations merely derived from the two data dimensions not presenting current surface conditions.

Here, four maps have been created using the grazing vulnerability index. On them, the high temporal resolution maps all show similar patterns with vulnerable areas in two corners of the map by the east side of the sample area. As previously described these areas are where the biomass is high and primary production low. When the same regions are inspected on the high spatial resolution images (Figure 13), these vulnerable patches are less visible and appear smaller and more dispersed. However, the vulnerable patches are dispersed over the same region between the different resolutions, although appearing less concentrated with higher detail.

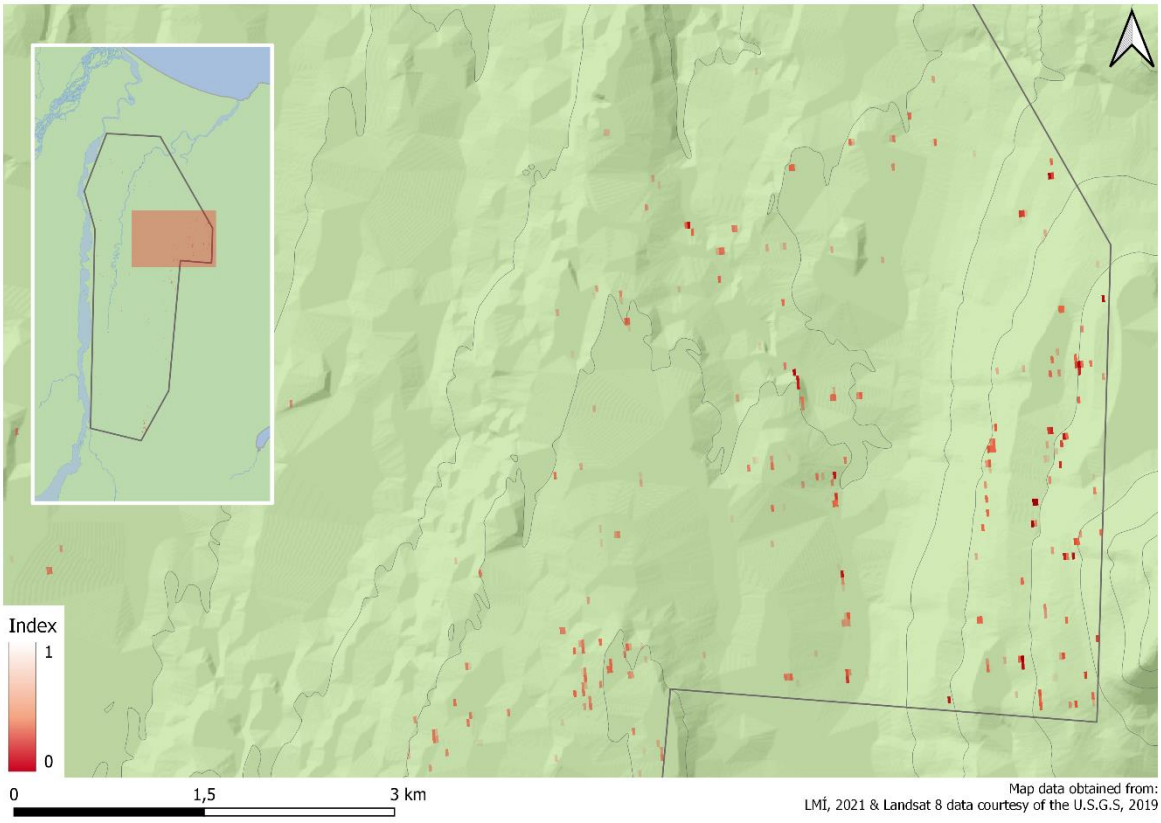

Figure 13: Detailed grazing vulnerability patterns observed with Landsat 8's high spatial resolution

Since all values below 0 have been removed from the NDVI dataset, non-vegetated pixels are presented as transparent on the index maps. Although they are not of concern to the index in a specific term, they must be considered in relation to overgrazing. When overgrazing occurs, the vegetation cover is removed, leaving bare ground. The NDVI value for bare ground is very likely to be less than 0.2 and can fall below 0. These bare ground pixels are then represented as transparent, or not visible, on the map and categorised here as not vulnerable which is only partly true. For overgrazed areas to recover new growth has to be left ungrazed for vegetation to re-establish (Arnalds, 2015). In their current state, they are not vulnerable to overgrazing because there is little vegetation which may be a result of overgrazing in the past.

From these results, vulnerability appears to be more likely correlated with elevation. The eastern side of the sample area, where most of the vulnerability is highlighted, is largely dissimilar from the rest by its increased elevation. Indeed, the easter side represents the eastern slopes of the valley in Úthérað. Moreover, climate influenced these results since the limiting factor to primary production in Iceland is often the short growing season. With elevation temperature decreases and weather is harsher, the vegetation in the highlands is therefore more vulnerable and prone to erosion, thus, more barren and sparsely or unvegetated (Arnalds, 2015). Indeed, on the Environment Agency of Iceland's biotope map (https://vistgerdakort.ni.is/), the vulnerable areas on the index map match the areas where barren and sparsely vegetated areas become more predominant in the heathlands. Here vegetation is less resilient and desertification is already occurring (Arnalds, 2015; Arnalds et al., 2001).

The results presented on the grazing vulnerability index maps do not allow an interpretation of the effect of overgrazing through reindeer presence (Figure 8 to Figure 11). However, it provides novel insights into where vegetation might be threatened by grazing. The low NDVI identified in this analysis shows areas of low primary production. In combination with the reindeer's high presence in the same area, this could mean that these areas are particularly prone to degradation (Bernes et al., 2015). Whether reindeer grazing pressure is the cause of the low primary production by the removal of vegetation or the cause of overgrazing is beyond the scope of this study and requires further investigation in the field. Nevertheless, since the measures of vegetation cover are one of the criteria for reindeer population management in Iceland, the grazing vulnerability index may be used as guidelines to these environmental management schemes. Areas highlighted by the index could targeted for monitoring land conditions, for example.

The satellites used had different properties resulting in varying advantages. Their spatial– and temporal resolution are considered to distinguish their advantages to the greatest degree, both suitable for studies such as this, but careful attention should be given to those attributes and related to what is to be observed. The data was free and publicly available and open–source software was only used for the study. The steps undertaken to generate a grazing vulnerability index have been outlined using this free software, so that practitioners can use them in planning and wildlife management. Commercial data and software are expensive and often requires specialist training but is suggested to be unnecessary for observing vegetation conditions in Iceland. Indeed, gathering free publicly available data and using free open software did not pose any difficulties for this study. Wildlife managers should develop semi–automatic routines for regular monitoring of the habitats using these results.

5.3 Summary

The analyses show differences in relation to the suitability of different satellites for studying grazing vulnerability by reindeer. These differences can be attributed to the satellites' spatial and temporal resolution making their suitability dependant on the scale of the subject area as well as the target of the study. The high spatial resolution satellites are convenient for observations of detailed changes of areas at risk of overgrazing, while high temporal resolution satellites can be used to detect more general patterns rapidly.

A grazing vulnerability index was generated and used to generate maps of the area of interest in this study. The index shows great promise in its applicability to environmental monitoring

as a counteraction to land degradation. Four maps were created using the index, one for each satellite used in the study. The grazing vulnerability index highlighted mainly two areas in the sample area by Úthérað that might be at risk of overgrazing. These areas highlighted are in higher elevation than most of the observed area, which is concurrent with previous research on the topic and might need to be further addressed to prevent overgrazing and land degradation.

6 Conclusion and outlook

This study aimed to assess the applicability of different satellite sensors to detect vulnerable areas to reindeer grazing using simple, cost-efficient remote sensing methods. The ecosystem impact of sheep overgrazing in Iceland is evident and has been thoroughly investigated (Arnalds, 2015). Grazing pressures in the Icelandic highlands has resulted in massive land degradation and soil erosion, which is deemed Iceland's biggest environmental problem. Research on the influence of wild herbivores, such as reindeer, is missing in Iceland, likely due to their much lower numbers and limited range as well as remote habitats. Indeed, their remote habitats make accurate observations of their grazing impacts on the vegetation difficult to monitor. Therefore, I suggested using recently generated biomass data by Boulanger-Lapointe (unpublished) as an indicator of their presence, thus, their grazing pressures, and comparing it to forage or phytobiomass data, in the form of satellite-derived primary productivity data, namely the NDVI. By doing map areas vulnerable to overgrazing by reindeer could be mapped using the grazing vulnerability index.

The uses of NDVI in previous studies, in relation to herbivores, reindeer and inter-trophic interactions were outlined, suggesting NDVI as an appropriate index for this study. The method used in this research was different from traditional methods which are often labour intensive, in the form of wildlife monitoring and require specialised analyses. Here I utilise the spatially associated biomass data and easily accessible NDVI to determine vulnerable areas to grazing pressure.

Different resolutions are crucial elements to consider prior to data collection. High temporal resolution can be suitable for a meso−macro scale study area or if relatively few cloud-free days are present over the study area. Although, the high temporal data is often made manageable with less computational capacity by sacrificing another resolution component such as spatial resolution. In certain observations, lower spatial resolution can aggregate too little of the observations so that it is less visible for optical observations. Lower spatial resolution can average out the relatively few pixels with relatively high values over a larger area, highlighting the properties of interest.

Likewise, high spatial resolution can be suitable for meso−macro scale areas but requires much computational capacity and optimal surface reflectance condition e.g., cloud-free day during the observational period. The high spatial resolution enables micro−meso scale observations that high temporal resolution is not capable of most often. Details are more visible with the high spatial resolution and relate better with patchy land degradation signal from the NDVI.

In this study, I established a procedure for detecting areas of vulnerable ecosystems to reindeer grazing. This was done by looking into spatially allocated forage availability and consumption. Those being biomass and NDVI, their values were normalised to be made relatable – being measured on different scales – or adjusted to a notionally common scale by dividing them with their maximum values so that their ratio could be calculated. The ratio contributes to the study as an index with a signal presenting forage availability and consumption, for and by reindeer. When the forage availability is low and the consumption is high the vegetation, being the forage, is at risk of overgrazing by reindeer. Overgrazing

risk being the focus of the study and the index's direct signal ranging from 0 to 1 presenting relative grazing vulnerability, the importance of the index is evident.

This index was named the grazing vulnerability index and was used to generate maps of the sample area to highlight vulnerable areas to overgrazing by reindeer. The index maps were made of a sample area to reduce the computational power required for larger data such as the high spatial resolution images. Finding high spatial resolution images was also problematic due to the rarity of cloud-free days concurring during the satellite's observation period. Thus, the sample area was determined by available cloud-free high spatial resolution images. The index maps show areas at risk to reindeer grazing since their presence there is high, likely resulting in high consumption, while the primary production in the same areas is low. I concluded that the areas highlighted by the index maps are mostly at higher elevation where growing conditions are poor.

Using the procedure described for the high temporal data over the species distribution range would provide a good overview of where the highest risk zones are for overgrazing pressure by reindeer. From there a high spatial resolution index could be created to narrow the vulnerable areas down to areas that should then be used for ground truthing observations. By doing so researchers could confirm the validity of the index maps as an indicator of vulnerable areas and establish protective measures for vegetation at risk.

A limitation to the grazing vulnerability index is the novelty of the metabolic biomass raster. Although similar studies have generated metabolic biomass rasters, the quantity of data used to determine their presence is enormous (Bubnicki et al., 2019). Boulanger-Lapointe's (unpublished) biomass raster has yet to be confirmed using ground-truthing data. The method is not habituated amongst scientists focusing on ecosystems and needs ground-truthing data to confirm the spatial patterns suggested by the herbivore maps.

I suggest that the grazing vulnerability index can be an essential tool for determining where ground-truthing measures can most effectively occur. The index maps show areas where vegetation conditions may be negatively affected by reindeer. Vulnerable areas highlighted by the index maps might be good indicators for where the herbivore map is well in sync with actual herbivore presence since the index highlights areas that are short of forage, possibly due to reindeer grazing pressures.

Finally, the NDVI preferences of reindeer suggested by the Landsat 8 scatter plot offers potential ecosystem information. If there is a NDVI signal preference by reindeer it could lead to easier detection of their presence where the signal is abundant. It can also be used to determine their habitat size for the population density calculations. Since their vegetated habitat area determines the population management it gives us a better understanding of the size of their preferred areas.

To determine whether there is a direct or indirect relationship between reindeer herd densities and plant productivity or health, several offsetting factors must be recognised such as climate variations on primary productivity, soil conditions, vegetation community composition, differences in rutting behavioural patterns, etc. (Bro-Jørgensen et al., 2008; Campeau et al., 2019). Furthermore, additional statistical analysis is required to assess these correlations' strengths while accounting for time-lagged effects. These measures are beyond the scope of this study and therefore a more straightforward objective was applied.

I suggest that further research establishes a method to determine whether overgrazing is occurring, using satellite data such as VIs. The areas highlighted here or by the same methodology over the whole reindeer distribution range would be well suited to determine a study area for this kind of research. This is made possible with my high temporal resolution data results being just as well suited for general vulnerability patterns as the high spatial resolution data. The high temporal resolution NDVI data available for the reindeer habitat area, is compatible and requires minimum computational capacity for a grazing vulnerability index map. It is free and publicly available data which would make it highly cost-effective, especially in combination with open software such as QGIS.

Grazing pressure by geese, ptarmigan and other wildlife is further highlighted by Þórisson (2018) and it will be important to include these species in environmental monitoring. If overgrazing pressure by wildlife is to be determined these grazers would need to be considered by a similar approach to evaluate each species pressure. From there wildlife management can be designed in a sustainable way.

References

Aradóttir, Á. L., & Arnalds, Ó. (2001). Ecosystem degradation and restoration of birch woodlands in Iceland. In F. E. Wielgolaski (Ed.), *Man and the Biosphere series* (pp. 293–306). Parthenon Publishing.

Arnalds, Ó. (2015). *the Soils of Iceland*. Springer. https://doi.org/10.1007/978-94-017-9621-7

Arnalds, Ó. (2020). *Ástand lands og hrun íslenskra vistkerfa*. Landbúnaðarháskóli Íslands. http://www.lbhi.is/sites/lbhi.is/files/gogn/vidhengi/rit_lbhi_nr_130_0.pdf

Arnalds, O., Þorarinsdottir, E. F., Metusalemsson, S., Jonsson, A., Gretarsson, E., & Arnason, A. (2001). *Soil Erosion in Iceland*. The Soil Conservation Service and the Agricultural Research Institute. http://hdl.handle.net/10802/9371

Asrar, G., Fuchs, M., Kanemasu, E. T., & Hatfield, J. L. (1984). Estimating Absorbed Photosynthetic Radiation and Leaf Area Index from Spectral Reflectance in Wheat. *Agronomy Journal*, *76*(2), 300-306. https://doi.org/10.2134/agronj1984.00021962007600020029x

Beamish, A., Raynolds, M. K., Epstein, H., Frost, G. V., Macander, M. J., Bergstedt, H., Bartsch, A., Kruse, S., Miles, V., Tanis, C. M., Heim, B., Fuchs, M., Chabrillat, S., Shevtsova, I., Verdonen, M., & Wagner, J. (2020). Recent trends and remaining challenges for optical remote sensing of Arctic tundra vegetation: A review and outlook. *Remote Sensing of Environment*, *246*, 111872. https://doi.org/10.1016/j.rse.2020.111872

Bernes, C., Bråthen, K. A., Forbes, B. C., Speed, J. D. M., & Moen, J. (2015). What are the impacts of reindeer/caribou (*Rangifer tarandus L.*) on arctic and alpine vegetation? A systematic review. *Environmental Evidence*, *4*(1), 4. https://doi.org/10.1186/s13750-014-0030-3

Björnsson, H., Sigurðsson, B. D., Davíðsdóttir, B., Ólafsson, J., Ástþórssson, Ó. S., Ólafsdóttir, S., Baldursson, T., & Jónsson, T. (2018). *Loftslagsbreytingarog áhrif þeirra á Íslandi: Skýrsla vísindanefndar um loftslagsbreytingar*. Veðurstofa Íslands.

Boulanger-Lapointe, N. (2021). Metabolic biomass data of reindeer [Unpublished data]. University of Iceland.

Bro-Jørgensen, J., Brown, M. E., & Pettorelli, N. (2008). Using the satellite-derived normalized difference vegetation index (NDVI) to explain ranging patterns in a lek-breeding antelope: the importance of scale. *Oecologia*, *158*(1), 177-182. https://doi.org/10.1007/s00442-008-1121-z

Bubnicki, J. W., Churski, M., Schmidt, K., Diserens, T. A., & Kuijper, D. P. (2019). Linking spatial patterns of terrestrial herbivore community structure to trophic interactions. *eLife*, *8*, e44937. https://doi.org/10.7554/eLife.44937

Campeau, A. B., Rickbeil, G. J. M., Coops, N. C., & Côté, S. D. (2019). Long-term changes in the primary productivity of migratory caribou (Rangifer tarandus) calving grounds and summer pasture on the Quebec-Labrador Peninsula (Northeastern Canada): the mixed influences of climate change and caribou herbivory. *Polar Biology*, *42*(5), 1005-1023. https://doi.org/10.1007/s00300-019-02492-6

Congedo, L. (2016). *Semi-automatic Classification Plugin documentation*. https://doi.org/10.13140/RG.2.2.29474.02242/1

DeFries, R. (2013). Remote Sensing and Image Processing. In S. A. Levin (Ed.), *Encyclopedia of Biodiversity (2nd ed.)* (pp. 389-399). Academic Press. https://doi.org/10.1016/B978-0-12-384719-5.00383-X

Didan, K. (2015). *MOD13Q1 MODIS/Terra Vegetation Indices 16-Day L3 Global 250m SIN Grid V006*. https://doi.org/10.5067/MODIS/MOD13Q1.006

Earth Explorer. (2000). U.S. Geological Survey. https://doi.org/10.3133/fs08300

Eckert, S., & Engesser, M. (2013). Assessing vegetation cover and biomass in restored erosion areas in Iceland using SPOT satellite data. *Applied Geography*, *40*, 179-190. https://doi.org/10.1016/j.apgeog.2013.02.015

Einarsson, M. Á. (1984). Climate in Iceland. In H. v. Loon (Ed.), *World Survey of Climatology* (Vol. 15, pp. 673-697). Elsevier. https://doi.org/10.1127/0941-2948/2007/0185

ESA. (n. d.). *Copernicus Sentinel*. https://sentinels.copernicus.eu/web/sentinel/home

Guðmundsdóttir, E. (2017). *Hreindýraveiðisvæði*. Náttúrustofa Austurlands. https://www.na.is/index.php/vefdyr

IPCC. (2014). *Climate Change 2014: Synthesis Report. Contribution of Working Groups I, II and III to the Fifth Assessment Report of the Intergovernmental Panel on Climate Change* (Core Writing Team, R. K. Pachauri, & L. A. Meyer, Eds.). IPCC. https://www.ipcc.ch/site/assets/uploads/2018/05/SYR_AR5_FINAL_full_wcover.pdf

Kristófersson, D., Runólfsson, S., Aradóttir, Á. L., Valsdóttir, E. H., Sigurðardóttir, S. F., Pétursson, J. G., & Arnalds, A. (2012). *Tillögur að inntaki nýrra laga um landgræðslu. Greinargerð starfshóps til umhverfisráðherra*. https://www.stjornarradid.is/media/umhverfisraduneyti-media/media/landgraedsluskyrsla-2012/landgraedslugreinargerd-lokautgafa-juli-2012.pdf

Landsat collection 2. (2021). U. S. Geological Survey. https://doi.org/10.3133/fs20213002

Lög um vernd, friðun og veiðar á villtum fuglum og villtum spendýrum nr.64/1994 https://www.althingi.is/lagas/nuna/1994064.html

Muhammad Aqeel Ashraf, Mohd. Jamil Maah, & Ismail Yusoff. (2010). Introduction to Remote Sensing of Biomass. In I. Atazadeh (Ed.), *Biomass and Remote Sensing of Biomass*. https://doi.org/10.5772/16462

Myneni, R. B., Hall, F. G., Sellers, P. J., & Marshak, A. L. (1995). The interpretation of spectral vegetation indexes. *IEEE Transactions on Geoscience and Remote Sensing*, *33*, 481-486. https://doi.org/10.1109/tgrs.1995.8746029

Myneni, R. B., & Williams, D. L. (1994). On the relationship between FAPAR and NDVI. *Remote Sensing of Environment*, *49*(3), 200-211. https://doi.org/10.1016/0034-4257(94)90016-7

Newton, E. J., Pond, B. A., Brown, G. S., Abraham, K. F., & Schaefer, J. A. (2014). Remote sensing reveals long-term effects of caribou on tundra vegetation. *Polar Biology*, *37*(5), 715-725. https://doi.org/10.1007/s00300-014-1472-3

Pettorelli, N., Vik, J. O., Mysterud, A., Gaillard, J.-M., Tucker, C. J., & Stenseth, N. C. (2005). Using the satellite-derived NDVI to assess ecological responses to environmental change. *Trends in Ecology & Evolution*, *20*(9), 503-510. https://doi.org/10.1016/j.tree.2005.05.011

QGIS Development Team. (2021). *QGIS Geographic Information System*. QGIS Association. https://www.qgis.org

R Core Team. (2017). *R: A Language and Environment for Statistical Computing*. R Foundation for Statistical Computing. https://www.R-project.org/

Raynolds, M., Magnússon, B., Metúsalemsson, S., & Magnússon, S. H. (2015). Warming, Sheep and Volcanoes: Land Cover Changes in Iceland Evident in Satellite NDVI Trends. *Remote Sensing*, *7*(8), 9492-9506. https://www.mdpi.com/2072-4292/7/8/9492

Raynolds, M., Walker, D. A., Epstein, H. E., Pinzon, J. E., & Tucker, C. J. (2012). A new estimate of tundra-biome phytomass from trans-Arctic field data and AVHRR NDVI. *Remote Sensing Letters*, *3*(5), 403-411. https://doi.org/10.1080/01431161.2011.609188

Rickbeil, G. J. M., Coops, N. C., & Adamczewski, J. (2015). The grazing impacts of four barren ground caribou herds (*Rangifer tarandus groenlandicus*) on their summer ranges: An application of archived remotely sensed vegetation productivity data. *Remote Sensing of Environment*, *164*, 314-323. https://doi.org/10.1016/j.rse.2015.04.006

Rouse, J., Haas, R. H., Schell, J. A., & Deering, D. (1974). *Monitoring vegetation systems in the great plains with ERTS* Third ERTS-1 Symp., Greenbelt. https://ntrs.nasa.gov/api/citations/19740022614/downloads/19740022614.pdf

Rumora, L., Miler, M., & Medak, D. (2021). Contemporary comparative assessment of atmospheric correction influence on radiometric indices between Sentinel-2A and Landsat 8 imagery. *Geocarto International*, *36*(1), 13-27. https://doi.org/10.1080/10106049.2019.1590465

Sundqvist, M. K., Moen, J., Björk, R. G., Vowles, T., Kytöviita, M.-M., Parsons, M. A., & Olofsson, J. (2019). Experimental evidence of the long-term effects of reindeer on Arctic vegetation greenness and species richness at a larger landscape scale. *Journal of Ecology*, *107*(6), 2724-2736. https://doi.org/10.1111/1365-2745.13201

Technical Support. (2020, June 5). ESRI. https://support.esri.com/en/technical-article/000005606

Þórarinsson, S. (1950). Náttúruvernd. Erindi flutt á 60 ára afmælisfundi Hins íslenska náttúrufræðifélags 31. október 1949. *Náttúrufræðingurinn*, *20*(1), 1-12.

Þórisson, S. (1983). *Hreindýrarannsóknir 1979 - 1981*. Náttúrustofa Íslands. https://orkustofnun.is/gogn/Skyrslur/OS-1983/OS-83072.pdf

Þórisson, S. G. (2018). *Population dynamics and demography of reindeer (Rangifer tarandus L.) on the East Iceland highland plateau 1940–2015 A comparative study of two herds* [Master's thesis, University of Iceland]. Reykjavík. http://hdl.handle.net/1946/30920

Þórisson, S. G., Þórarinsdóttir, R., & Ágústsdóttir, K. (2021). *Vöktun hreindýra 2020 og tillaga um veiðikvóta og ágangssvæði 2021* (NA-210206). Náttúrustofa Austurlands. https://www.na.is/images/stories/utgefid/2021-2022/NA-210206_Voktun_hreindyra_2020_og_tillaga_ad_veidikvota_og_agangssvaedi_2021.pdf

U.S. Geological Survey. (n. d.). *Landsat Missions*. https://www.usgs.gov/core-science-systems/nli/landsat

Veðurstofa Íslands. (2019a, 1. July). *Tíðarfar í júlí 2019*. https://vedur.is/um-vi/frettir/tidarfar-i-juli-2019

Veðurstofa Íslands. (2019b, 1. June). *Tíðarfar í júní 2019*. https://vedur.is/um-vi/frettir/tidarfar-i-juni-2019

Wickham, H. (2009). *ggplot2: Elegant Graphics for Data Analysis*. Springer-Verlag. http://ggplot2.org

Yengoh, G. T., Dent, D., Olsson, L., Tengberg, A. E., & III, C. J. T. (2016). *Use of the Normalized Difference Vegetation Index (NDVI) to Assess Land Degradation at Multiple Scales: Current Status, Future Trends, and Practical Considerations*. Springer books. https://doi.org/10.1007/978-3-319-24112-8